

Ditopic receptors containing urea groups for solvent extraction of Cu(II) salts[†]

Israel Carreira-Barral^a, Marta Mato-Iglesias^a, Andrés de Blas^a, Carlos Platas-Iglesias^a, Peter A. Tasker^b and David Esteban-Gómez^a

^a Universidade da Coruña, Centro de Investigacións Científicas Avanzadas (CICA) and Departamento de Química Fundamental, Facultade de Ciencias, 15071, A Coruña, Galicia, Spain

^b The School of Chemistry at Edinburgh, West Mains Road, Edinburgh, EH9 3JJ, UK

Dalton Transactions Volume 46, Issue 10, pages 3192–3206, 14 March 2017

Received 10 January 2017, Accepted 15 February 2017, First published 15 February 2017

How to cite:

Ditopic receptors containing urea groups for solvent extraction of Cu(II) salts. I. Carreira-Barral, M. Mato-Iglesias, A. de Blas, C. Platas-Iglesias, P. A. Tasker and D. Esteban-Gómez, *Dalt. Trans.*, 2017, **46**, 3192–3206. DOI: [10.1039/C7DT00093F](https://doi.org/10.1039/C7DT00093F).

Abstract

The ditopic receptor **L**³ [1-(2-((7-(4-(tert-butyl)benzyl)-1,4,7,10-tetraazacyclododecan-1-yl)methyl)phenyl)-3-(3-nitrophenyl)urea] containing a macrocyclic cyclen unit for Cu(II)-coordination and a urea moiety for anion binding was designed for recognition of metal salts. The X-ray structure of [Cu**L**³(SO₄)] shows that the sulfate anion is involved in cooperative binding via coordination to the metal ion and hydrogen-bonding to the urea unit. This behaviour is similar to that observed for the related receptor **L**¹ [1-(2-((bis(pyridin-2-ylmethyl)amino)methyl)phenyl)-3-(3-nitrophenyl)urea], which forms a dimeric [Cu**L**¹(μ-SO₄)₂] structure in the solid state. In contrast, the single crystal X-ray structure of [Zn**L**³(NO₃)₂] contains a 1 : 2 complex (metal : anion) where one anion coordinates to the metal and the other is hydrogen-bonded to the urea group. Spectrophotometric titrations performed for the [Cu**L**³(OSMe₂)₂]²⁺ complex indicate that this system is able to bind a wide range of anions with an affinity sequence: MeCO₂⁻ > Cl⁻ > H₂PO₄⁻ > Br⁻ > NO₂⁻ > HSO₄⁻ > NO₃⁻. Lipophilic analogues of **L**¹ and **L**³ extract CuSO₄ and CuCl₂ from water into chloroform with high selectivity over the corresponding Co(II), Ni(II) and Zn(II) salts.

Keywords: hydrometallurgy; anion recognition; copper(II) complexes; ditopic ligands; solvent extraction experiments; urea moiety

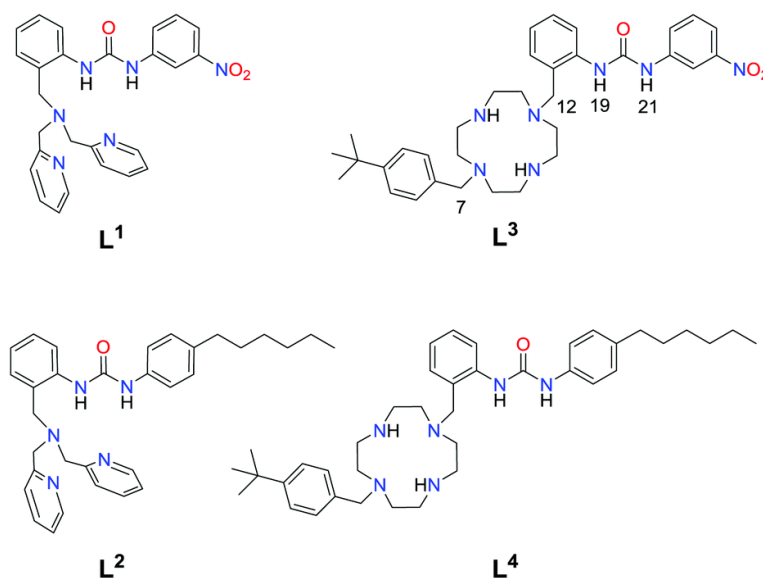
Introduction

Modern hydrometallurgical processes employ solvent extraction to separate and concentrate targeted metals after the dissolution of ores in aqueous media.^{1,2} Frequently the extractants generate anionic ligands that form hydrophobic charge-neutral complexes with the targeted metal ion.³ Alternatively, the migration of the metal ion to the organic phase may be aided by the simultaneous recognition of attendant anions, transferring a metal salt. For instance, extraction of CuCl₂ and ZnCl₂ can be achieved by using appropriate extractants that form charge neutral complexes of the form [CuCl₂L₂] or [Zn₂Cl₄L₂],^{4,5} where L represents the extractant. Application of this strategy to the extraction of metal sulfates is more challenging due to the weak coordinating ability of this anion and its high hydration energy.⁶ This makes it energetically less favourable to transfer sulfate into a hydrophobic medium than monoanions such as chloride or nitrate (the Hofmeister

bias).⁷ Consequently, the extraction of metal sulfates from aqueous solutions requires developing alternative strategies.

The most successful approach to achieve selective extraction of sulfate salts relies on the use of ditopic receptors that possess two well-defined binding sites for the metal cation and the sulfate anion. Metal salt recognition may occur either independently or through cooperative binding involving the coordination of the anion to the metal ion and the synergistic interaction of the anion with the ditopic ligand through hydrogen bonds. Among the anion recognition units incorporated into ditopic metal salt receptors are amides,⁸ ammonium,⁹ guanidinium,¹⁰ pyrrol,¹¹ urea¹² and thiourea¹³ groups.

In previous work we showed that the binding of an anion to a Cu(II) complex of the ditopic receptor **L**¹ is cooperative, involving both coordination of the anion to the copper ion and hydrogen bonding with the urea unit of the ligand.¹⁴ The binding of SO₄²⁻ generates a charge-neutral complex that could be exploited for the extraction of CuSO₄. Herein we report an analogue **L**² with a hydrophobic hexyl chain replacing the nitro group and two new ditopic ligands, **L**³ and **L**⁴, which are based on a cyclen unit which is expected to increase the stability of the corresponding Cu(II) complexes as the stability constant reported for [Cu(cyclen)]²⁺ (log K₁₁ = 23.4)^{15,16} is ten orders of magnitude higher than that for [Cu(dpa)]²⁺ (dpa = di(2-picoly)amine, log K₁₁ = 13.8).¹⁷ Furthermore, Cu(II) complexes with cyclen derivatives generally form complexes with square pyramidal coordination environment, where the basal plane is defined by the four nitrogen atoms of the macrocycle and the apical position is occupied by an additional ligand.¹⁸ This feature should provide easy access for a coordinating anion which is then well placed to interact with the urea anion-acceptor. The ability of [Cu**L**³]²⁺ to bind anions through cooperative interactions, investigated using spectrophotometric titrations, and solvent extraction studies to assess the potential of **L**² and **L**⁴ to extract different Cu(II) salts are reported below.



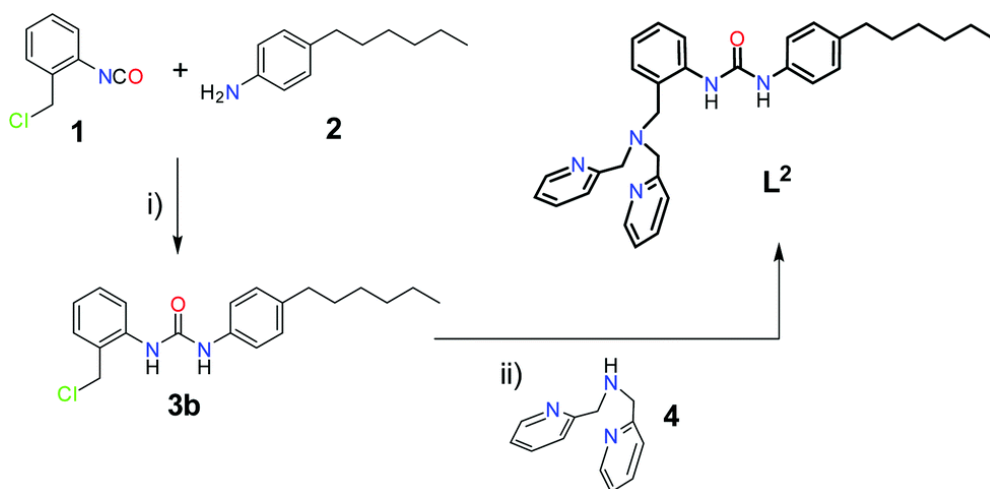
Scheme 1. Structures of the ligands **L**¹⁻⁴ investigated in this work.

Results and discussion

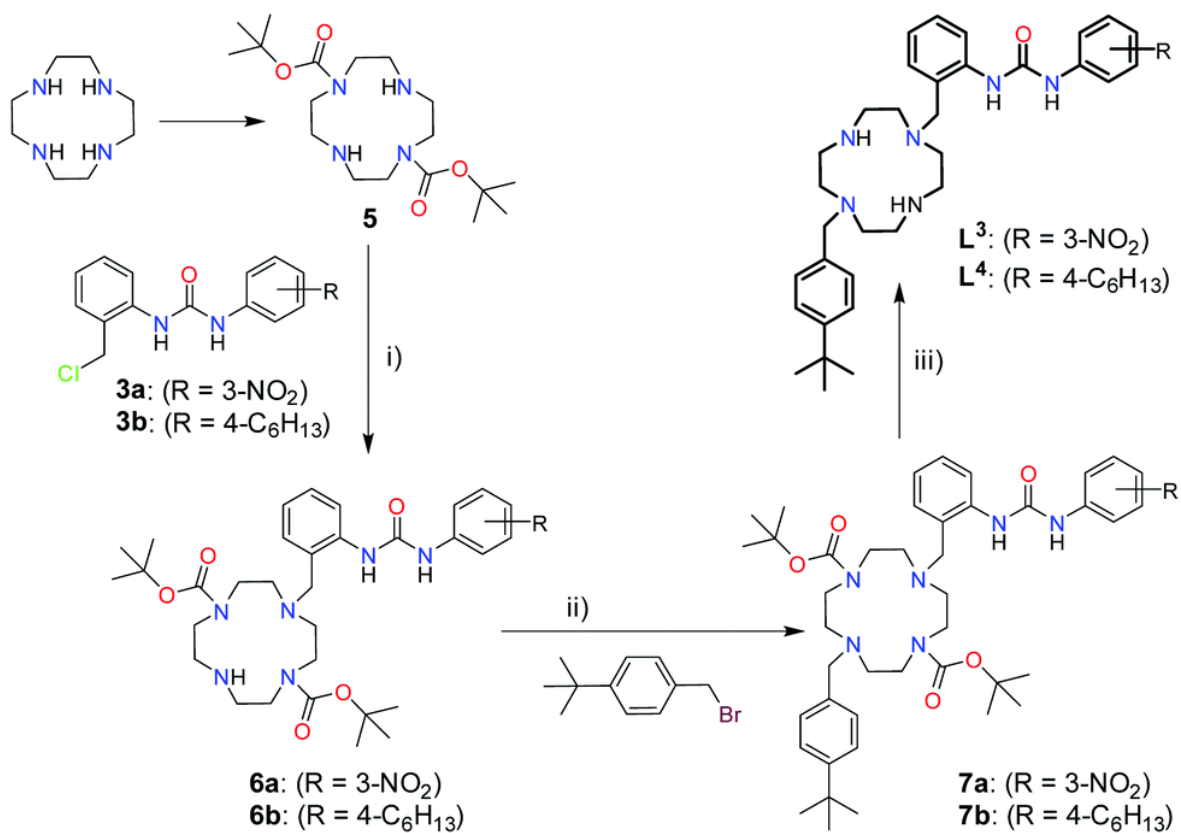
Synthesis of the ligands

Full experimental details are provided in the ESI.† **L**² was obtained using a procedure (Scheme 2) similar to that for **L**¹.¹⁴ The syntheses of **L**³ and **L**⁴ involved the monoalkylation of diBoc-cyclen¹⁹ (**5**) with either **3a** or

3b using a fivefold excess of **5** to avoid the formation of the dialkylated product. Reaction of **6a** and **6b** with 1-(bromomethyl)-4-(*tert*-butyl)benzene gave **7a** and **7b** in moderate yields (~54%) which were deprotected quantitatively using a 1 : 1 mixture of chloroform and trifluoroacetic acid (Scheme 3).



Scheme 2. Synthesis of L^2 . Reagents and conditions: (i) Et₂O, r.t., 48 h; (ii) CH₃CN, dipea, KI (cat.), Δ , 72 h.



Scheme 3. Synthesis of L^3 and L^4 . Reagents and conditions: (i) CH₃CN, K₂CO₃, r.t., 16 h; (ii) CH₃CN, dipea, KI (cat.), Δ , 16 h; (iii) CHCl₃:tfa (1 : 1), r.t., 16 h.

The structure of L^3 was confirmed by X-ray diffraction (Fig. 1). The conformation of the macrocycle in the solid state is defined by the formation of intramolecular hydrogen bonds between the urea NH groups and two nitrogen atoms of the macrocyclic fragment [N(3)⋯N(4), 2.900(2) Å, N(3)–H(3N)⋯N(4) 140(2)°; [N(3)⋯N(5), 3.379(2) Å, N(3)–H(3N)⋯N(5) 144(1)°; N(2)⋯N(5), 2.902(2) Å, N(2)–H(2N)⋯N(5) 172(2)°]. An additional intramolecular hydrogen bond involves the two secondary amine nitrogen atoms of the cyclen moiety [N(5)⋯N(6), 3.441(2) Å, N(5)–H(5N)⋯N(6) 171(1)°]. The 12-membered macrocycle adopts a square [3333] conformation in which the ligand is predisposed to bind metal ions.²⁰

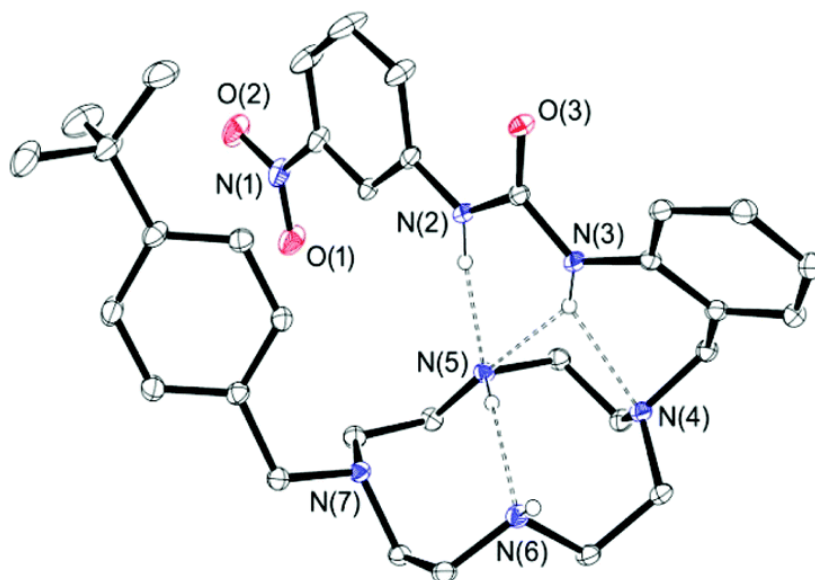


Fig. 1. View of the X-ray structure of L^3 . Hydrogen atoms bonded to carbon are omitted for clarity. The thermal parameters in this and Fig. 2–4 are plotted at the 30% probability level.

Synthesis and characterization of the metal complexes

Prior to the isolation of solid complexes, the coordination of L^3 to Cu(II) was investigated using spectrophotometric titrations in acetonitrile solution (Fig. S1, ESI†). The absorption spectrum of L^3 shows an intense band at 261 nm ($\epsilon = 40\,363\text{ M}^{-1}\text{ cm}^{-1}$) characteristic of the diphenylurea chromophore²¹ together with a weak absorption at 350 nm ($\epsilon = 1900\text{ M}^{-1}\text{ cm}^{-1}$) attributed to the $-\text{NO}_2$ group in *meta* position with respect to the urea unit. Addition of $\text{Cu}(\text{OTf})_2$ is accompanied by hypsochromic shifts of the two absorption bands. The titration profile shows a single inflection point and three isosbestic points at 210, 252 and 280 nm that are consistent with a 1 : 1 stoichiometry (Fig. S1, ESI†).

Reaction of L^3 with one equivalent of MCl_2 or hydrated $\text{M}(\text{NO}_3)_2$, $\text{M}(\text{ClO}_4)_2$ and $\text{M}(\text{SO}_4)$ ($\text{M} = \text{Cu}$ or Zn) in methanol at room temperature yielded the desired complexes isolated as the corresponding chloride, perchlorate, nitrate or sulfate salts in 59–88% yields.

Slow evaporation of solutions of $[\text{Cu}L^3(\text{SO}_4)] \cdot 1.5\text{H}_2\text{O}$ and $[\text{Zn}L^3(\text{NO}_3)_2] \cdot \text{CHCl}_3$ in chloroform/methanol or acetonitrile/methanol afforded single crystals suitable for X-ray structure determination of formula $[\text{Cu}L^3(\text{SO}_4)] \cdot \text{MeOH}$ and $[\text{Zn}L^3(\text{NO}_3)]\text{NO}_3 \cdot 0.75\text{MeOH}$, respectively. Structures are shown in Fig. 2 and 3, and bond distances in the inner coordination spheres are listed in Table 1. The coordination polyhedron around the Cu(II) ion in $[\text{Cu}L^3(\text{SO}_4)] \cdot \text{MeOH}$ can be described as a square pyramid, the donor atoms of the cyclen fragment [N(4), N(5), N(6) and N(7)] defining the basal plane and one of the oxygen atoms of the sulfate anion [O(4)] occupying the apical position (Fig. 2). The metal ion is located 0.55 Å above the basal

plane (mean deviation from planarity: 0.03 Å). The *cis* angles of this plane, ranging between 84.1° and 86.8°, are slightly smaller than 90° due to the displacement of the metal ion from the basal plane. For the same reason the O(4)–Cu(1)–N angles deviate up to 22° from 90° (Table S1, ESI†), while the *trans* angles fall in the range 146.1–150.8°. The index of trigonality τ amounts to 0.08, which is in agreement with a square pyramidal geometry.²² The distances between the heteroatoms of the cyclen subunit and the Cu(II) ion are similar to those reported for other five-coordinated Cu(II) complexes containing cyclen.²³ The four five-membered chelate rings formed upon coordination of the cyclen fragment adopt identical conformations, which results in the (δδδδ) [or (λλλλ)] conformation of the macrocyclic unit often observed in the solid state for metal complexes with cyclen-based ligands.²⁴

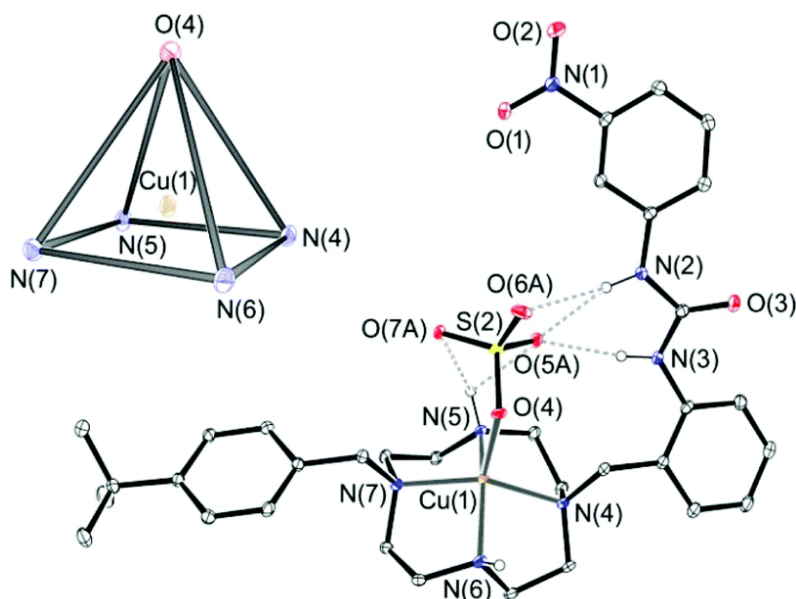


Fig. 2. The X-ray structure of [CuL³(SO₄)]. Hydrogen atoms bonded to carbon atoms are omitted for clarity. The inset shows a representation of the square pyramidal coordination polyhedron.

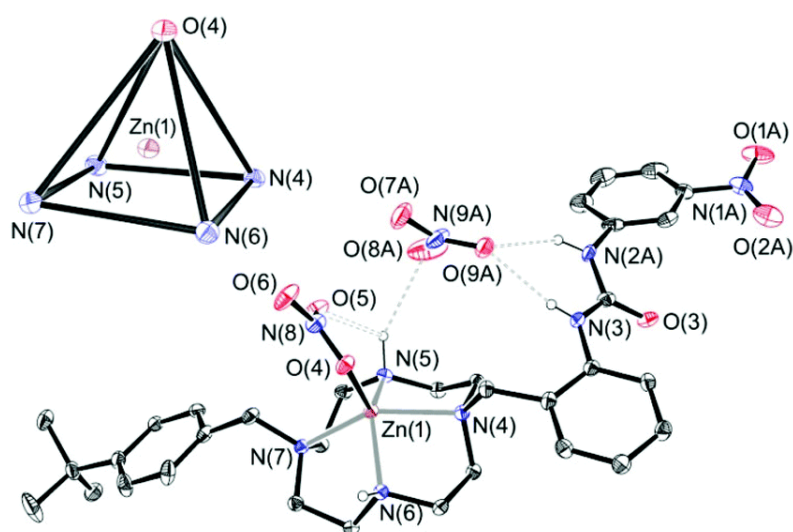


Fig. 3. The X-ray structure of [ZnL³(NO₃)](NO₃). Hydrogen atoms bonded to carbon atoms are omitted for clarity. The uncoordinated nitrate ion and the distal part of the urea moiety show positional disorder with occupation factor of 0.613(8) for atoms labelled with A.

Table 1. Bond distances (Å) of the metal coordination spheres in [CuL³(SO₄)]·MeOH, [ZnL³(NO₃)](NO₃)·0.75MeOH and [CuL¹(μ-SO₄)]₂·C₆H₆N₂O₂

	[CuL ³ (SO ₄)]	[ZnL ³ (NO ₃)]NO ₃	[CuL ¹ (μ-SO ₄)] ₂ ^a
M(1)–N(3)			3.007(1)
M(1)–N(4)	2.083(2)	2.228(2)	2.032(2)
M(1)–N(5)	2.001(2)	2.088(3)	1.998(2)
M(1)–N(6)	2.019(2)	2.093(2)	1.980(2)
M(1)–N(7)	2.071(2)	2.188(3)	
M(1)–O(4)	2.150(2)	1.989(2)	1.939(1)
M(1)–O(7)#1			2.327(1)

^aSymmetry transformations used to generate equivalent atoms: #1 $-x + 1, -y + 1, -z + 1$.

The coordinated sulfate anion in [CuL³(SO₄)]·MeOH forms three comparably strong hydrogen bonds with the NH groups of the urea, N(2) and N(3). Additional weak hydrogen bonds involve the oxygen atoms of the sulfate group O(5A) and O(7A) and the secondary amine nitrogen atom N(5) of the cyclen unit (Table 2).

Table 2. Some intramolecular hydrogen bonds in [CuL³(SO₄)]·MeOH, [ZnL³(NO₃)](NO₃)·0.75MeOH and [CuL¹(μ-SO₄)]₂·C₆H₆N₂O₂

[CuL ³ (SO ₄)] ^a	$d(D\cdots A)/\text{Å}$	$d(H\cdots A)/\text{Å}$	D–H \cdots A/ $^\circ$	S(2)–O \cdots H/ $^\circ$
N(2)–H(2N) \cdots O(6A)	3.117(7)	2.29	155.8	97.6
N(2)–H(2N) \cdots O(5A)	3.121(6)	2.38	142.0	93.0
N(3)–H(3N) \cdots O(5A)	2.917(4)	2.08	159.7	128.7
N(5)–H(5N) \cdots O(5A)	2.961(7)	2.39	115.5	89.0
N(5)–H(5N) \cdots O(7A)#1	2.968(5)	2.27	126.1	79.0
[ZnL ³ (NO ₃)](NO ₃) ^b	$d(D\cdots A)/\text{Å}$	$d(H\cdots A)/\text{Å}$	D–H \cdots A/ $^\circ$	N(9A)–O \cdots H/ $^\circ$
N(2A)–H(2A) \cdots O(9A)	3.09(4)	2.13(11)	149(7)	131.9
N(3)–H(3N) \cdots O(9A)	2.87(2)	2.08(6)	161(5)	153.3
N(5)–H(5N) \cdots O(5)	2.978(4)	2.47(5)	120(4)	116.4
N(5)–H(5N) \cdots O(8A)#1	3.351(13)	2.62(5)	148(9)	
[CuL ¹ (μ-SO ₄)] ₂	$d(D\cdots A)/\text{Å}$	$d(H\cdots A)/\text{Å}$	D–H \cdots A/ $^\circ$	S(1)–O \cdots H/ $^\circ$
N(2)–H(2N) \cdots O(6)	2.959(2)	2.14(2)	172(2)	102.6
N(3)–H(3N) \cdots O(5)	2.790(2)	1.99(2)	169(2)	102.2

^aSymmetry transformations used to generate equivalent atoms: #1 $-x, -y, -z$. ^bSymmetry transformations used to generate equivalent atoms: #1 $x + 3/2, y + 1/2, -z + 3/2$ #2 $-x + 3/2, -y + 3/2, -z + 1$ #3 $-x + 3/2, y - 1/2, -z + 3/2$ #4 $x + 1/2, y - 1/2, z + 1$.

Crystals of [ZnL³(NO₃)]NO₃·0.75MeOH contain a five coordinate Zn(II) ion directly bound to the four nitrogen atoms of the macrocycle and an oxygen atom of a coordinated nitrate anion (Fig. 3). The metal coordination environment can be best described as square-pyramidal ($\tau = 0.15$), with the basal plane of the pyramid (mean deviation from planarity: 0.057 Å) being defined by the four donor atoms of the cyclen fragment [N(4), N(5), N(6) and N(7)]; the apical position is occupied by an oxygen atom of the coordinated nitrate anion [O(4)]. The Zn(1)–O(4) distance (1.989(2) Å) is *ca.* 0.1–0.2 Å shorter than those between the Zn(II) ion and the nitrogen atoms of the basal plane (Table 1). These bond distances are similar to the ones

reported for other five-coordinated Zn(II) complexes containing cyclen.²⁵ The metal ion is located 0.76 Å above the basal plane, resulting in *cis* angles in the range 81.86–84.00°, and angles defined by the Zn(1)–O(4) vector and the donor atoms of the basal plane of 106.1–120.0°.

Unlike in [CuL³(SO₄)], the coordinated anion does not interact with the urea group in [ZnL³(NO₃)](NO₃). Instead, the coordinated nitrate anion establishes a weak intramolecular hydrogen-bonding interaction with the N(5)–H(5N) group of the cyclen subunit (Table 2). The uncoordinated nitrate anion forms an asymmetrical and bifurcated hydrogen bond with the urea moiety. The D···A distances and D–H···A angles characterizing this interaction point to hydrogen bonds with a moderate strength (Table 2). The N(9A)–O(9A)···H(2A) and N(9A)–O(9A)···H(3N) angles (126.8° and 149.3°, respectively) are relatively close to the ideal value of 115 ± 10°.²⁶

In previous work we reported the X-ray structure of the blue mononuclear complex [CuL¹(SO₄)(H₂O)],¹⁴ which crystallised from an aqueous solution. The same solution also provided green crystals which contain the dimeric, centrosymmetric and charge-neutral [CuL¹(μ-SO₄)₂] entity and a molecule of 3-nitroaniline, presumably arising from the hydrolysis of the urea unit (Fig. 4). The metal coordination environment is approximately square pyramidal, where the basal plane is defined by the three donor atoms of the dpa unit and an oxygen atom of the coordinated sulfate anion [O(4)]. The oxygen atom of a second sulfate anion [O(7)] coordinates at the apical position. The Cu(1)–O(7) distance (2.327(1) Å) is considerably longer than those involving donor atoms of the basal plane (1.94–2.03 Å, Table 1). The nitrogen atom of the urea unit N(3) provides a weak interaction with the Cu(II) ion (Cu(1)–N(3) = 3.007(1) Å), as observed for [CuL¹(SO₄)(H₂O)]. The two sulfate anions act as η₁:η₁:μ₂ bridging ligands, a coordination mode observed previously in different binuclear Cu(II) complexes.^{27,28} The intramolecular Cu(1)···Cu(1') distance is 4.3914(4) Å.

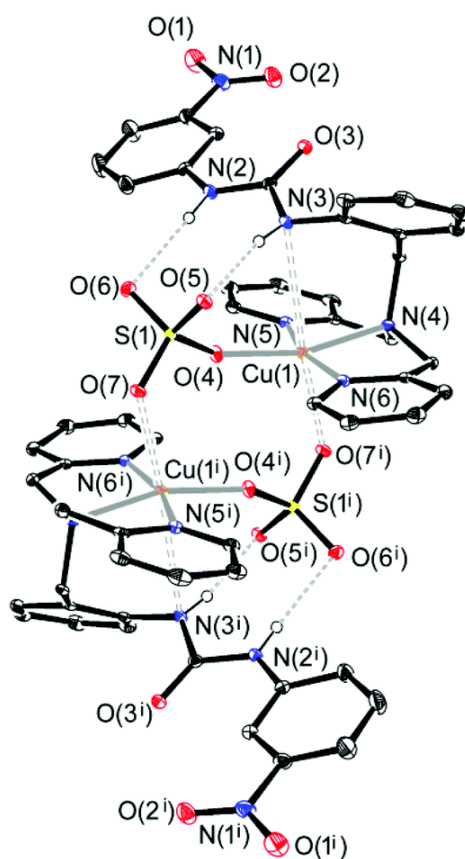


Fig. 4. View of the X-ray structure of [CuL¹(μ-SO₄)₂]. Hydrogen atoms bonded to carbon atoms are omitted for clarity.

The structural features of $[\text{CuL}^1(\mu\text{-SO}_4)]_2$ (Table 2) point to stronger and more directional interactions of the sulfate anion with the urea group than in $[\text{CuL}^3(\text{SO}_4)]$. Thus, the two N–H \cdots O contacts in $[\text{CuL}^1(\mu\text{-SO}_4)]_2$ show similar distances and angles and the S(1)–O(6)–H(2N) and S(1)–O(5)–H(3N) angles are close to the ideal value ($122 \pm 12^\circ$).²⁹ In $[\text{CuL}^3(\text{SO}_4)]$ the S(1)–O(6) \cdots H(2N) angle (97.6°) deviates considerably from the ideal value, most likely as a consequence of the simultaneous binding to the N–H groups of the cyclen moiety.

NMR studies

The ^1H NMR spectrum of $[\text{ZnL}^3](\text{ClO}_4)_2$ shows signals at 9.36 and 8.13 ppm due to the urea protons H19 and H21 (Fig. 5, see Scheme 1 for labelling). The chemical shifts in the free receptor are very different (8.47 and 9.93 ppm for H19 and H21, respectively), which likely reflects the disruption of the intramolecular hydrogen bonds involving the urea unit upon coordination of the ligand to the metal ion (Fig. 1). In the presence of more readily coordinating anions such as Cl^- or NO_3^- important changes are observed. The resonance of H21 experiences a strong deshielding, while that of H19 undergoes a slight upfield shift, reflecting the establishment of hydrogen-bonding interactions between the anion and the N–H fragments of the urea moiety. Two sets of signals with relative intensities of 2 : 3 and 1 : 3 are observed for $[\text{ZnL}^3](\text{NO}_3)_2$ and $[\text{ZnL}^3]\text{Cl}_2$, pointing to the presence of two different species in solution in slow exchange on the NMR timescale. The nature of the solvent (dmsO) is important in defining these isomers (^1H and ^{13}C NMR spectra recorded in CD_3CN solution are in agreement with the presence of a single complex species in solution (Fig. S2, ESI †)). Thus, the two species observed in dmsO solution are attributed to $[\text{ZnL}^3\text{X}]^+$ and $[\text{ZnL}^3(\text{OSMe}_2)\cdots\text{X}]^+$ species ($\text{X} = \text{Cl}^-$ or NO_3^-), in which the anion is involved in hydrogen bonding interaction with the urea unit and either coordinated or non-coordinated to the metal ion. The lower coordinating character of CH_3CN favours the exclusive formation of the $[\text{ZnL}^3\text{X}]^+$ species. The ^1H NMR data therefore reveal that the anions interact with the urea moiety *via* hydrogen bonds, but exclude the coordination of the urea nitrogen atom to the metal ion, as observed for $[\text{ZnL}^1](\text{ClO}_4)_2$.¹⁴ DFT calculations (TPSSH/TZVP)³⁰ performed on the $[\text{ZnL}^3\text{Cl}]^+$ system in dmsO solution (IEFPCM)³¹ support the simultaneous binding of the anion to the metal ion and the urea unit (Fig. S3, ESI †).

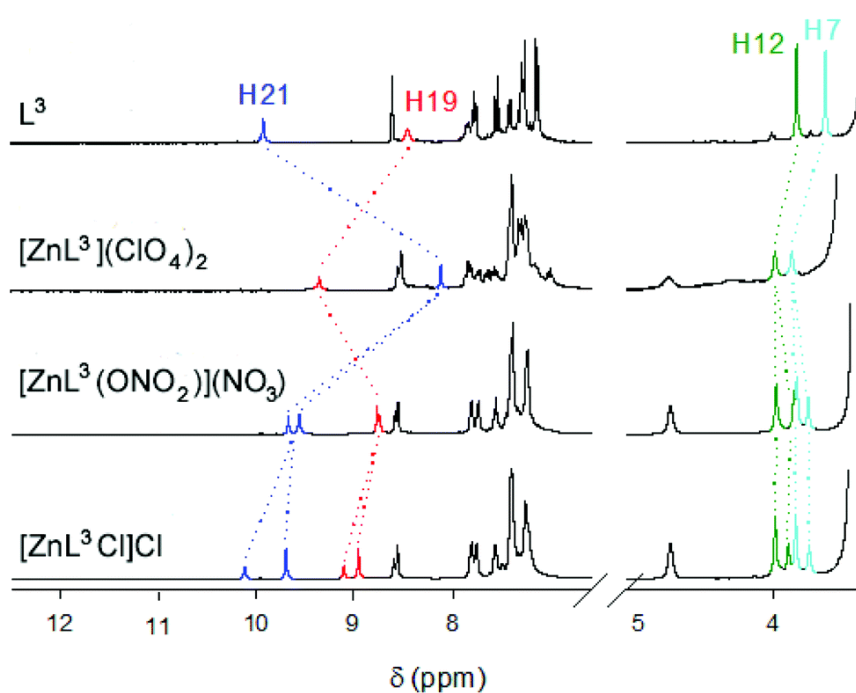


Fig. 5. ^1H NMR spectra (300 MHz, 25 °C, $\text{dmsO-}d_6$) of L^3 and its Zn(II) complexes.

Anion-binding studies

Before investigating the interaction of the Cu(II) complex of L^3 with NO_3^- , HSO_4^- , $H_2PO_4^-$, NO_2^- , $MeCO_2^-$, F^- , Cl^- and Br^- (as their tetrabutylammonium salts), the interaction of the free ligand with these anions was studied. Spectrophotometric titrations, monitored using the CT band centred on the nitro group, show that only $MeCO_2^-$ and F^- are able to compete with the solvent in forming hydrogen-bonds with the receptor (as previously observed with L^1 (Fig. S4, ESI†)). The smooth curvature of the titration profiles, which prevented an accurate calculation of the association constants, indicates that these interactions are weak. This might be attributed to the presence of intramolecular hydrogen bonds between the urea moiety and the nitrogen atoms of the ligand, which are likely stronger than those involving the urea group and the anions (Fig. 1).

The absorption spectrum of $[CuL^3(OSMe_2)]^{2+}$ has a broad band (500–1200 nm with a maximum at 621 nm, $\epsilon = 341 \text{ M}^{-1} \text{ cm}^{-1}$) characteristic of d–d transitions centred on the Cu(II) ion and is very similar to that in the five-coordinated cyclen complex $[Cu(\text{cyclen})(NCMe)](W_6O_{19})$.^{32a} Such bands are attributed to the $d_{xz}, d_{yz} \rightarrow d_x^2 - y^2$ (${}^2B_1 \rightarrow {}^2E$) transition expected for a square-pyramidal geometry (Fig. 6) and DFT calculations on dmsO solutions are consistent with the square pyramidal coordination provided is fulfilled by the four nitrogen atoms of the cyclen unit and an apical solvent (dmsO) molecule (Fig. S3, ESI†). Attempts to optimise the $[CuL^3]^{2+}$ system with one of the nitrogen atoms of the urea unit coordinated to the metal ion resulted in its systematic expulsion from the metal's inner coordination sphere.

Solutions of $[CuL^3(OSMe_2)]^{2+}$ in dmsO (prepared by dissolution of perchlorate salt) were titrated with stock solutions of the anions as their tetrabutylammonium salts in the same solvent (10^{-3} M and 0.1 M , respectively). Anion interaction was monitored by following the variations in the d–d band of the Cu(II) ion. Addition up to a 20-fold excess of NO_3^- is accompanied by only small changes in the absorption spectrum, which indicates a very weak binding of this anion to the metal complex. In contrast, addition of HSO_4^- causes a slight red shift of the d–d band and its intensity slightly decreases (Fig. 6a). However, a reliable association constant could not be determined given the slight curvature of the titration profile.

Addition of $H_2PO_4^-$, NO_2^- , $MeCO_2^-$, $PhCO_2^-$, Cl^- or Br^- to solutions of $[CuL^3(OSMe_2)]^{2+}$ in dmsO causes significant changes in the d–d absorption band of the complex (Fig. 6, see also Fig. S5, ESI†); anion addition provokes a red shift of the d–d band of 48–98 nm and its intensity decreases slightly (Table 3), which is in agreement with the position of the dmsO ligand in the spectrochemical series with respect to the employed anions.^{32b} The shape of the d–d absorption band does not change upon anion addition, which suggests that the square pyramidal coordination is retained. The titrations with $H_2PO_4^-$, NO_2^- , Cl^- and Br^- present a single inflection point with two clear isosbestic points, consistent with the formation of 1 : 1 complexes. The equilibrium constant determined for the interaction with Cl^- ($\log K_{11} = 5.57(2)$) is higher than that with Br^- ($\log K_{11} = 4.22(3)$), which is in agreement with the higher stability of Cu(II) complexes with Cl^- and the better hydrogen-bonding acceptor character of Cl^- compared to Br^- .³³ The association constants determined for the interaction of $[CuL^3(OSMe_2)]^{2+}$ with Cl^- and Br^- are lower than those obtained for $[CuL^1(OSMe_2)_2]^{2+}$ (Table 3).

The equilibrium constant $\log K_{11}$ determined for NO_2^- ($\log K_{11} = 3.65(3)$) is lower than that measured previously for $[CuL^1(OSMe_2)_2]^{2+}$ ($\log K_{11} = 5.46(9)$). In the latter the NO_2^- is coordinated to the metal ion in a bidentate fashion. However, $[CuL^3(OSMe_2)]^{2+}$ presents only one coordination position available for anion binding. Consequently only a monodentate coordination mode of an anion is possible, explaining weaker binding. The higher value of $\log K_{11}$ obtained for $H_2PO_4^-$ in $[CuL^3(OSMe_2)]^{2+}$ compared to $[CuL^1(OSMe_2)_2]^{2+}$ is perhaps a consequence of a stronger interaction of this anion with the urea moiety, since in $[CuL^3(OSMe_2)]^{2+}$ the urea group, unlike in $[CuL^1(OSMe_2)_2]^{2+}$, is not coordinated to the metal ion.

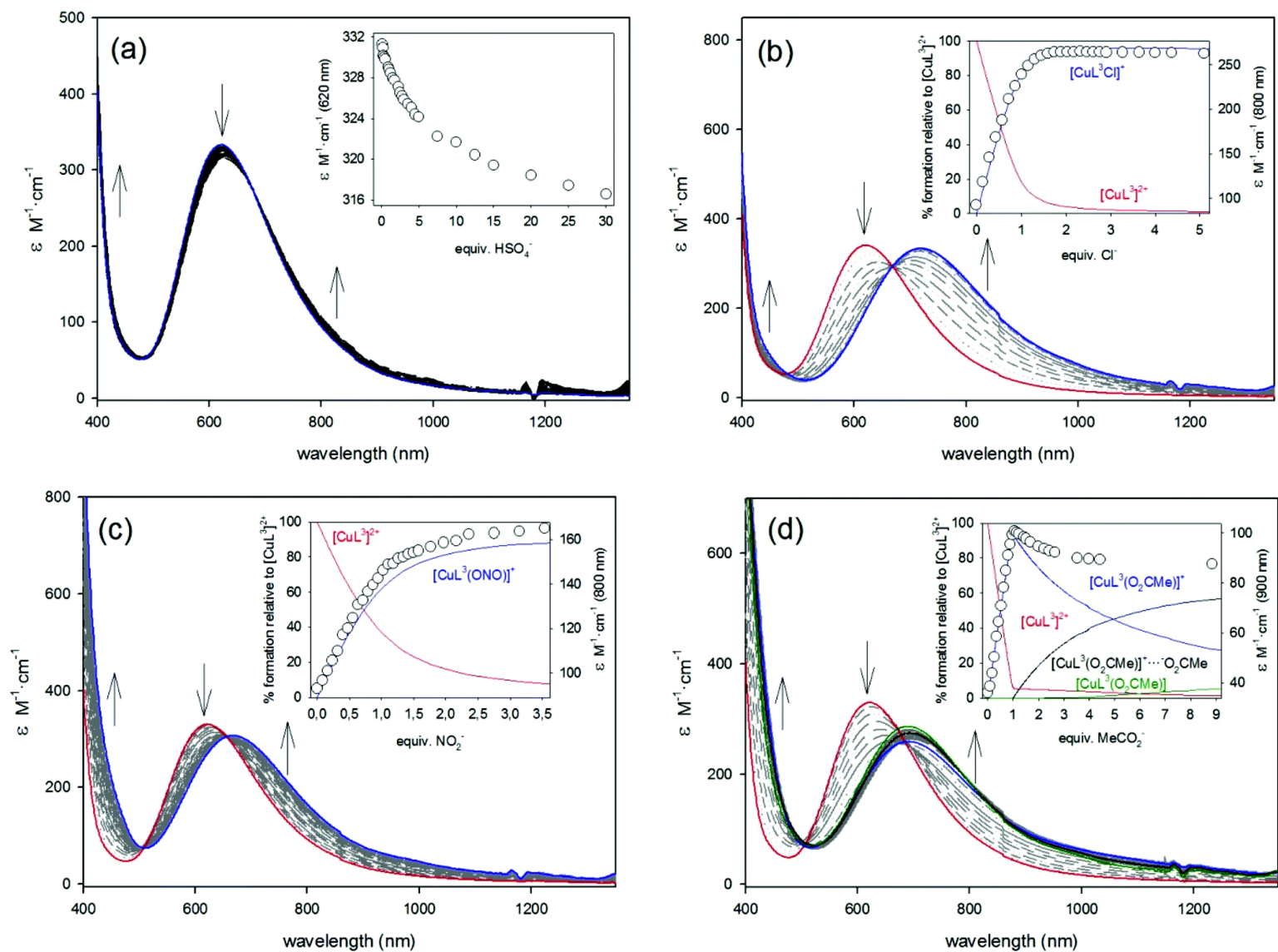


Fig. 6. UV/vis spectra recorded during the titration of $[\text{CuL}^3(\text{OSMe}_2)]^{2+}$ (10^{-3} M in dmsO) with a standard solution (0.1 M in dmsO, 25 °C) of: (a) $[\text{Bu}_4\text{N}]\cdot\text{HSO}_4^-$; (b) $[\text{Bu}_4\text{N}]\cdot\text{Cl}^-$; (c) $[\text{Bu}_4\text{N}]\cdot\text{NO}_2^-$ and (d) $[\text{Bu}_4\text{N}]\cdot\text{MeCO}_2^-$. Insets: titration profiles at selected wavelengths vs. equivalents of anion and species distribution diagram (coordinated dmsO molecules are omitted for clarity).

Table 3. Spectroscopic data and association constants (log K values) obtained from spectrophotometric titrations in dmsO solution.

Anion	$[\text{CuL}^3(\text{OSMe}_2)]^{2+}$		$[\text{CuL}^1(\text{OSMe}_2)_2]^{2+}$ ^a	
	log K_{11}	$\lambda_{\text{max}}(\text{nm})$	log K_{11}	$\lambda_{\text{max}}(\text{nm})$
HSO_4^-	<2	628	3.36(9)	679
H_2PO_4^-	5.09(5)	684	3.81(4)	684
NO_2^-	3.65(3)	669	5.46(9)	630
MeCO_2^-	>7	692	>7	653
PhCO_2^-	>7	674	>7	652
F^-	>7	688	>7	695
Cl^-	5.57(2)	719	>7	680
Br^-	4.22(3)	705	3.81(6)	679

^a Data taken from ref. 14.

Addition of up to 1 equiv. of MeCO_2^- or PhCO_2^- to a solution of $[\text{CuL}^3(\text{OSMe}_2)]^{2+}$ leads to a more pronounced decrease in the intensity of the d–d absorption band centred at 621 nm (Fig. 6, see also Fig. S5, ESI†), reflecting monodentate binding of the anion to the metal ion. The formation of the 1 : 1 adducts is characterised by higher stability constants (log $K > 7$). The intensity of the band increases until a second equiv. of the anion has been added, in agreement with the formation of a hydrogen-bond adduct involving the urea group and the anion, as observed in the solid state for $[\text{ZnL}^3(\text{NO}_3)]\text{NO}_3 \cdot 0.75\text{MeOH}$ (Fig. 3). The equilibrium constant (log $K = 2.7(1)$) for this step is lower than the values reported for other N,N' -substituted ureas in the same solvent.³⁴ This might be related to the strength of the hydrogen-bonding interaction or to a competitive process between the coordinated and the uncoordinated anions for the urea moiety. Further addition of anion promotes the deprotonation of the urea group with concomitant formation of a hydrogen-bond complex between acetate and its conjugated acid,³⁵ a process that is complete only after addition of a large excess of anion. When the titration is carried out at a lower concentration of complex (10^{-4} M; see Fig. S6, ESI†) a CT band at 366 nm centred on the nitro group develops. This results from the deprotonation of the N–H group closest to the 3-nitrophenyl substituent. The analysis of the titration data for $[\text{CuL}^3(\text{OSMe}_2)]^{2+}$ provides a $\text{p}K_a$ value of 13.4(3), considerably higher than the one determined for the L^1 derivative,¹⁴ where the urea fragment is N -coordinated to the metal ion. However, the urea group in $[\text{CuL}^3(\text{OSMe}_2)]^{2+}$ is more acidic than that of 1-(3,5-bis(trifluoromethyl)phenyl)-3-phenylurea,³⁶ most probably as a consequence of the polarisation of one of the N–H fragments caused by its interaction with the coordinated anion. Addition of PhCO_2^- to a solution of $[\text{CuL}^3(\text{OSMe}_2)]^{2+}$ provokes similar changes in the absorption spectrum, yielding $\text{p}K_a = 13.54(4)$.

The spectrophotometric titration of $[\text{CuL}^3(\text{OSMe}_2)]^{2+}$ with F^- reveals two different processes. The first involves the interaction of a F^- anion with the urea moiety through hydrogen bonding, while the second, observed only after addition of a large excess of anion, involves the deprotonation of the N–H fragment adjacent to the 3-nitrophenyl group (Fig. S5, ESI†).

The log K_{11} values obtained for the different anions (Table 3) follow the order $\text{MeCO}_2^- > \text{Cl}^- > \text{H}_2\text{PO}_4^- > \text{Br}^- > \text{NO}_2^- > \text{HSO}_4^- > \text{NO}_3^-$. For MeCO_2^- , PhCO_2^- and F^- the steep curvature of the titration profiles indicates especially high equilibrium constants (log $K_{11} > 7$). In contrast, NO_3^- and HSO_4^- interact only weakly with the complex. The observed sequence of anion affinity does not follow that expected according to the solvation terms; small anions such as Cl^- should be highly solvated, and the endothermic desolvation term should disfavour binding to the metal ion.³⁷ The association constants log K_{11} determined for MeCO_2^- , Cl^- and H_2PO_4^- are likely related to a cooperative effect between the coordinatively unsaturated metal ion

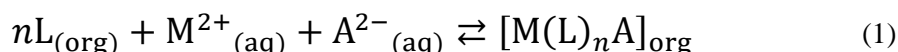
and the urea subunit, which is involved in a hydrogen-bonding interaction with the anion, reinforcing the binding to the Cu(II) ion.

Solvent extraction studies

Liquid–liquid extraction studies were carried out to investigate whether the hydrophobic ligands L^2 and L^4 were able to transport transition metal salts from water into chloroform.³⁸ In all the experiments a solution of the ligand in chloroform (10^{-3} M) was stirred for 16 h with an aqueous solution of Cu(II) or Zn(II) sulfate or chloride in the presence of an excess of sodium sulfate or chloride (0.6 M) and analysed as described in the ESI.†

Preliminary studies with L^2 and copper salts suggested that the receptor is only able to extract significant amounts of $CuCl_2$ and $CuSO_4$, as indicated by the colour intensity of the organic phase (see Fig. S7, ESI†). In the case of L^4 extraction of $CuSO_4$ was judged to be more favourable than $CuCl_2$ and $Cu(NO_3)_2$. In some cases a third phase developed during the extractions of the latter, which made it impossible to ensure a materials balance when recording the metal distribution between the organic and aqueous phases. Consequently extraction experiments were performed using sulfates and chlorides of Co(II), Ni(II), Cu(II) and Zn(II). No uptake of Co(II) and Ni(II) into the organic phase was observed from either sulfate or chloride solutions. Consequently the solvent extraction studies described below involve Cu(II) and Zn(II) salts.

Solvent extraction of a metal salt of a divalent anion A^{2-} is represented by eqn (1).



In the presence of a large excess of anion its concentration is effectively constant in the aqueous phase and the extraction equilibrium constant, K_e , and the distribution coefficient, D , are defined by eqn (2) and (3).

$$K_e = \frac{[M(L)_nA]_{(org)}}{[L]_{(org)}^n [M^{2+}]_{(aq)}} \quad (2)$$

$$D = \frac{[M(L)_nA]_{(org)}}{[M^{2+}]_{(aq)}} \quad (3)$$

The molar ratio (n parameter)³⁹ and the equilibrium constant of the extraction process (K_e)⁴⁰ (see eqn (4)) can then be determined from the slope and the intercept of the straight lines that should be obtained after fitting the experimental data of the plots of $\log D$ versus $\log[L]$.

$$\log D = n \log[L] + \log K_e \quad (4)$$

Plots of the uptake of CuSO_4 by L^2 and L^4 (Fig. S8, ESI†), performed in the presence of excess Na_2SO_4 at $\text{pH} = 5.5$,⁴¹ yield a value of $n \sim 1$, which is in agreement with the molecular structures of $[\text{CuL}^1(\text{SO}_4)(\text{OH}_2)]$,¹⁴ $[\text{CuL}^1(\mu\text{-SO}_4)]_2$ and $[\text{CuL}^3(\text{SO}_4)]$. Extraction of copper sulfate from acidic media is particularly relevant to commercial operations.^{1b,c} The $\log K_e$ values obtained from the intercepts (Fig. S8, ESI†) are 3.2(3) for L^2 and 3.6(2) for L^4 , indicating that the two ligands display similar extraction ability.

The pH dependence of uptake of CuSO_4 by L^2 and L^4 is shown in Fig. 7. For L^2 the Cu-loading is constant, $59 \pm 3\%$, across the pH range 0–5.5. In contrast, for L^4 no Cu(II) uptake is observed below $\text{pH} \sim 2$, and above this pH the amount of Cu(II) extracted increases, reaching a maximum of $49 \pm 3\%$ above $\text{pH} 4$. Two features of the loading behaviour were not expected. The formation constant in water for the cationic Cu-complex $[\text{Cu}(\text{cyclen})]^{2+}$ is nearly ten orders of magnitude higher than for the dpa analogue, $[\text{Cu}(\text{dpa})]^{2+}$, ($\log K_{11}$ values are 23.4 and 13.8 respectively),^{42,43} and whilst the proton affinity of cyclen is also higher ($\log K = 10.6$ and 9.6)⁴⁴ than that of dpa ($\log K = 7.3, 2.6$ and 1.1)⁴⁵ it is not sufficiently so to account for it appearing more favourable for Cu^{2+} to displace protons from the binding site of dpa than for cyclen. In an extraction experiment it may be the case that the stability of the salts $(\text{LH}_n)(\text{HSO}_4)_n$ or $(\text{LH}_n)(\text{SO}_4)_{n/2}$ in the organic phase is significantly higher for L^4 than for L^2 making it more difficult to displace protons by Cu^{2+} . Another factor which would impact on these loading data is the relative solubility of the protonated and copper-complexed forms of the ligands. The high hydration energy of the sulfate anion will influence this greatly, together with the observation that in water cyclen is expected to be present in its doubly protonated form below $\text{pH} \sim 9.6$, while the diprotonated form of dpa dominates the speciation in solution only below $\text{pH} 3.0$ (see Fig. S9, ESI†).

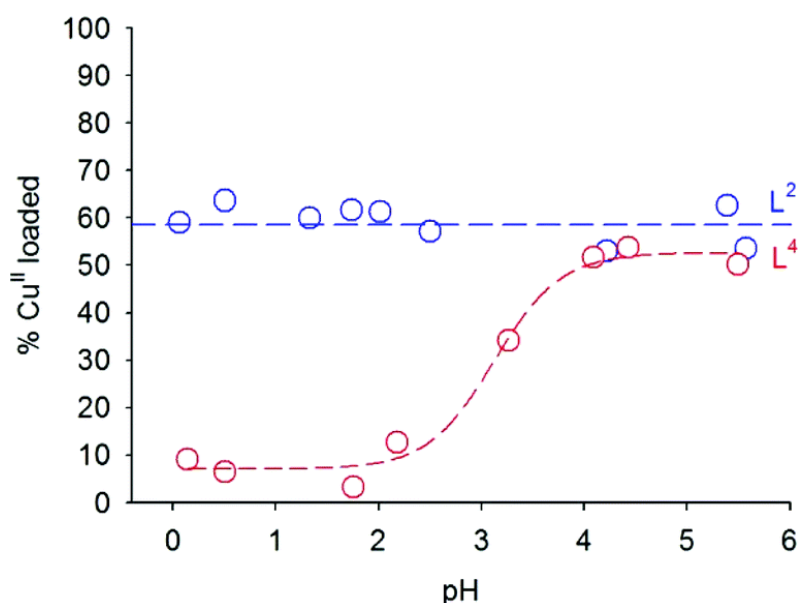


Fig. 7. pH profiles for Cu(II) loading by 10^{-3} M CHCl_3 solutions of L^2 and L^4 ligands from equal volumes of 10^{-3} M aqueous CuSO_4 .

The other unexpected feature of the pH-profiles for Cu uptake is the maximum loading of copper by L^4 being only *ca.* 50% of theory for the formation of $[\text{CuL}^4(\text{SO}_4)]$. The dependence of uptake on the concentration of CuSO_4 in water ($\text{pH} 5.5$) is shown in Fig. 8a. This confirms that the maximum uptake is $48 \pm 2\%$ and also shows that loading is independent of the concentration of CuSO_4 in the aqueous phase. In contrast, for L^2 20 equiv. of CuSO_4 is needed to reach a ‘plateau’ in which 70% of Cu is loaded. The dependence of loading on sulfate concentration (see Fig. 8b) is also very different for L^2 and L^4 with the Cu-uptake by L^4 ($53 \pm 2\%$)

varying very little whilst that by L^2 increases significantly and approaches that for L^4 when 600 equivalents of Na_2SO_4 have been added to the aqueous phase. The origins of the remarkable differences in behaviour of L^2 and L^4 in transporting $CuSO_4$ into chloroform are unclear. The similarity of the coordination chemistry shown by their analogues, L^1 and L^3 , in a single solvent and in the solid state (see above) suggests that differences in the relative stabilities and solubilities of their sulfate salts and copper sulfate complexes in the two solvents contribute to the unusual behaviour in solvent extraction experiments.

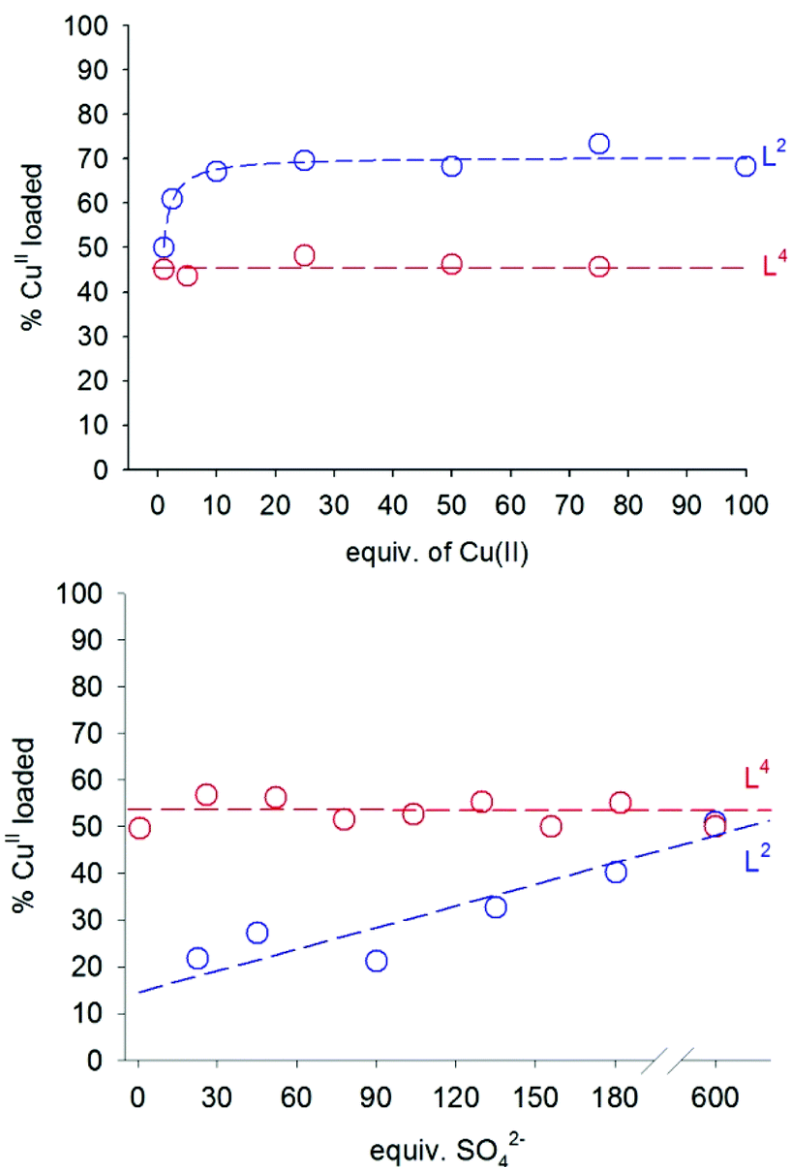


Fig. 8. Loadings of $CuSO_4$ by 10^{-3} M $CHCl_3$ solutions of L^2 and L^4 as a function on the $Cu(II)$ concentration (top) and the sulfate concentration (bottom) in the aqueous phase (pH = 5.5).

When a mixed metal aqueous solution of $Co(II)$, $Ni(II)$, $Cu(II)$ and $Zn(II)$ as their sulfates (10^{-3} M, pH 5.5) was contacted a chloroform solution (10^{-3} M) of L^2 or L^4 , only $CuSO_4$ was extracted suggesting that they could provide useful selectivity in hydrometallurgical concentration and separation of copper. Whilst acid stripping to recover the copper from L^4 should be possible (see Fig. 7), practicable reagents will need to have better loading efficiencies and better solubility in hydrocarbon diluents to merit development.

Preliminary tests showed that L^2 and L^4 were capable of extracting Zn(II) as well as Cu(II) from chloride solutions (no Co(II) or Ni(II) were loaded). A precipitate separated in extractions of $CuCl_2$ by L^4 , so studies of the efficiency of extraction and of the stoichiometry of complex formation in chloroform used only L^2 and allowed comparison with results for sulfate solutions. Loadings as a function of pH, Cu concentration and anion concentration are provided in Fig. S11, ESI.† A higher maximum loading of $CuCl_2$ ($91 \pm 2\%$) than of $CuSO_4$ ($70 \pm 2\%$) was observed as might be expected, given the chloride ion's lower hydration energy and better metal ligating properties. As for the sulfate systems, the stoichiometries of complex formation in chloroform are not consistent with maximum loadings. A plot of $\log D$ vs $\log[L]$ (Fig. S8, ESI†) has a slope of ~ 2 and the consequent 2 : 1 molar ratio of L^2 to Cu(II) indicates that the maximum loading should be 50%. It is probable that a mixture of species is transferred to the organic phase (the $\log D$ vs. $\log[L]$ plot is slightly curved). One of these species might be the $[CuL^2Cl_2]$ neutral complex⁴⁶ as mass spectra (Fig. S10, ESI†) show that both $[CuL^2Cl]^+$ and $[L^2 + Cl]^-$ species are present in solution, together with $([Cu(L^2)_2Cl]^+)$, which might exhibit a structure similar to that reported by Glerup *et al.*⁴⁷ The formation of several species which display different metal/ligand ratios during extraction has been previously reported by Ohmuro *et al.*^{39d}

The influence of pH and of the concentration of copper and of chloride on Cu(II) loading was investigated following similar procedures to those described for sulfate. The amount of Cu(II) loaded into the organic phase ($90 \pm 3\%$) is not affected by pH (in the range 0 to 5.5), nor by the concentration of Cu(II). In contrast, the uptake of copper is very dependent on the concentration of chloride in the aqueous phase and 60 equivalents are required to reach the 'plateau' in which 90% loading.

Only copper was extracted from an aqueous solution containing equimolar concentrations of Co(II), Ni(II), Cu(II) and Zn(II) chlorides, showing the same selectivity pattern as that observed for extraction from sulfate media.

Conclusions

The ditopic ligand L^3 containing a cyclen unit for cation binding and a urea motif for anion recognition has been prepared and characterised. X-ray crystal structures of $CuSO_4$ complexes show that SO_4^{2-} anion is involved in cooperative binding with simultaneous coordination of the anion to the metal ion and hydrogen-bonding to the urea subunit. In contrast, the NO_3^- anions in $[ZnL^3(NO_3)_2]$ do not show cooperative binding as one interacts only with the zinc ion, and the second is involved only in hydrogen-bonding with the urea moiety.

Spectrophotometric and 1H NMR titrations of the formation of the $[CuL^3(OSMe_2)]^{2+}$ complex and its Zn(II) analogue show that all investigated anions bind to the coordinatively unsaturated metal ion in dmsO solution with an affinity sequence $MeCO_2^- > Cl^- > H_2PO_4^- > Br^- > NO_2^- > HSO_4^- > NO_3^-$. Addition of large excesses of relatively basic anions such as $MeCO_2^-$ and F^- results in the deprotonation of the urea group, as evidenced by the charge transfer bands developed in the absorption spectra.

The ability of L^1 and L^3 to form stable metal salt complexes in solution and in the solid state is also found in solvent extraction experiments using their lipophilic analogues, L^2 and L^4 . Whilst these reagents show evidence for highly selective extraction of Cu(II) in the presence of Co(II), Ni(II) and Zn(II), their loading capacities are not sufficient to allow operation of efficient hydrometallurgical recovery processes. Investigation of the mechanisms of extraction suggest that more than one complex is formed in the organic phase and indicate that more lipophilic versions would be needed to develop efficient metal recovery processes.

Experimental section

Materials

1-(Chloromethyl)-2-isocyanatobenzene (**1**), 4-hexylaniline (**2**), bis(pyridin-2-ylmethyl)amine (**4**), 1,4,7,10-tetraazacyclododecane, 1-(bromomethyl)-4-(*tert*-butyl)benzene and *tert*-butyl-(oxycarbonyloxy)succinimide were obtained from commercial sources. Solvents were of reagent grade and used without further purification.

Caution: Although we have experienced no difficulties with the perchlorate salts, these should be regarded as potentially explosive and handled with care.

General methods

Elemental analyses were carried out on a ThermoQuest Flash EA 1112 elemental analyser. ESI-TOF mass spectra were recorded from MeOH/CH₂Cl₂/MeCN, MeOH/MeCN, MeCN, MeOH, MeOH/H₂O/MeCN or MeOH/MeCN/CHCl₃ solutions, using a LC-Q-q-TOF Applied Biosystems QSTAR Elite spectrometer in the positive mode. IR spectra were recorded using a Bruker Vector 22 spectrophotometer equipped with a Golden Gate attenuated total reflectance (ATR) accessory (Specac). ¹H and ¹³C NMR spectra were recorded at 25 °C on Bruker Avance 300 and Bruker Avance 500 spectrometers, and spectral assignments (see Scheme S1, ESI†) were based in part on 2D COSY, HSQC and HMBC experiments. UV/vis spectra were recorded with a Perkin-Elmer Lambda 900 spectrophotometer; those performed in solution were recorded with quartz cells (path length: 1 cm) and the cell holder was thermostated at 25.0 °C, through circulating water. Anion binding studies were performed by monitoring the spectral changes of a 10⁻³ M solution of complex [CuL³(ClO₄)₂] \cdot 2H₂O in dmsO upon addition of a 0.1 M solution of the corresponding tetrabutylammonium salt. Binding constants were obtained by using a simultaneous fit of the UV/vis absorption spectral changes at 7–12 selected wavelengths in the range 500–1200 nm. A minimum of 26 absorbance data points at each of these wavelengths was used, and all spectrophotometric titration curves were fitted with the HYPERQUAD program.⁴⁸

1-(2-(Chloromethyl)phenyl)-3-(4-hexylphenyl)urea (3b). A solution of 1-(chloromethyl)-2-isocyanatobenzene (**1**) (0.700 mL, 5.076 mmol) and 4-hexylaniline (**2**) (1.088 mL, 5.076 mmol) in diethyl ether (100 mL) was stirred at room temperature for 48 h. The precipitate formed was isolated by filtration and washed with diethyl ether (3 \times 10 mL) to give 1.533 g of the desired compound (88%) as a white solid. ¹H NMR (500 MHz, dmsO-*d*₆, 298 K): δ 9.41 (s), 9.35 (s), 8.38 (m), 8.26 (s), 7.88 (m), 7.41–7.37 (m), 7.34–7.28 (m), 7.26–7.17 (m), 7.08 (d, ³*J* = 8.2 Hz), 7.05–7.02 (m), 6.98 (m), 6.89 (m), 5.67 (s), 5.25 (s), 4.86 (s), 4.53 (s), 2.58 (m), 2.49 (m), 1.52 (m), 1.25 (m), 0.84 (m). ¹³C NMR (125.8 MHz, dmsO-*d*₆, 298 K): δ 153.0, 152.9, 152.0, 142.8, 137.8, 137.5, 137.5, 136.5, 135.9, 135.7, 131.4, 131.3, 130.7, 129.6, 129.3, 129.1, 128.8, 128.6, 128.6, 128.1, 127.5, 127.5, 125.7, 125.1, 124.5, 123.2, 123.0, 122.5, 122.3, 121.3, 118.6, 118.3, 113.8, 69.9, 67.6, 60.9, 43.7, 34.8, 34.7, 34.6, 31.3, 31.2, 31.2, 31.0, 28.5, 28.4, 28.3, 22.2, 22.2, 14.1, 14.1. MS-ESI⁺, *m/z* (%BPD): [**3** + H]⁺, 345.2 (1%); [**3** - Cl]⁺, 309.2 (100%). Elem. Anal. Calcd for C₂₀H₂₅ClN₂O: C, 69.7; H, 7.3; N, 8.1%. Found: C, 69.7; H, 6.8; N, 8.0%. IR: 3286 ν (N–H), 2958, 2925, 2853 ν (C–H), 1641 ν (C=O), 1606, 1588, 1487, 1450 ν (C=C), 1548 δ (N–H), 669 ν (C–Cl) cm⁻¹.

1-(2-((Bis(pyridin-2-ylmethyl)amino)methyl)phenyl)-3-(4-hexylphenyl)urea (L²). A solution of compound **3b** (0.923 g, 2.677 mmol), bis(pyridin-2-ylmethyl)amine (**4**) (0.452 mL, 2.434 mmol), *N,N*-diisopropylethylamine (0.848 mL, 4.868 mmol) and a catalytic amount of KI in acetonitrile (50 mL) was heated to reflux with stirring for 3 days. The resulting solution was filtered while hot and the filtrate concentrated to dryness. The residue was extracted with chloroform (5 \times 50 mL) and water (25 mL), the organic layer combined and dried over anhydrous Na₂SO₄, and the solvent evaporated under reduced pressure. The resulting oil was purified on a CombiFlash RF-200, using a 12 g-silica gel column and CH₂Cl₂ as eluent to obtain pure product L² as a pale yellow oil (0.631 g, 50%). ¹H NMR (500 MHz, CDCl₃,

298 K): δ 10.80 (s, 1H, H14), 8.85 (s, 1H, H16), 8.53 (ddd, 2H, H1, $^3J = 4.9$ Hz, $^4J = 1.7$ Hz, $^4J = 0.8$ Hz), 8.35 (m, 1H, H12), 7.56 (td, 2H, H3, $^3J = 7.7$ Hz, $^4J = 1.8$ Hz), 7.53 (m, 2H, H18), 7.27–7.24 (m, H4 and H11), 7.16–7.12 (m, 3H, H2 and H19), 7.07 (m, 1H, H9), 6.88 (td, 1H, H10, $^3J = 7.4$ Hz, $^4J = 1.2$ Hz), 3.85 (s, 4H, H6), 3.70 (s, 2H, H7), 2.57 (m, 2H, H21), 1.62 (m, 2H, H22), 1.39–1.26 (m, 6H, H23, H24 and H25), 0.90 (m, 3H, H26). ^{13}C NMR (125.8 MHz, CDCl_3 , 298 K): δ 158.0 C5, 153.4 C15, 149.3 C1, 140.2 C13, 137.9 C17, 137.0 C3, 136.8 C20, 130.0 C9, 129.0 C19, 128.8 C11, 124.2 C4, 124.1 C8, 122.7 C2, 121.3 C10, 119.1 C12, 118.6 C18, 59.7 C6, 58.5 C7, 35.4 C21, 31.9 C23, 31.7 C22, 29.1 C24, 22.7 C25, 14.2 C26. MS-ESI $^+$, m/z (%BPI): [$\text{L}^2 + \text{Na}$] $^+$, 530.3 (24%); [$\text{L}^2 + \text{H}$] $^+$, 508.3 (100%). Elem. Anal. Calcd for $\text{C}_{32}\text{H}_{37}\text{N}_5\text{O}\cdot 0.5\text{H}_2\text{O}$: C, 74.4; H, 7.4; N, 13.6%. Found: C, 74.9; H, 7.6; N, 13.5%. IR: 3330–3190 $\nu(\text{N-H})$, 3118–2853 $\nu(\text{C-H})$, 1705 $\nu(\text{C=O})$, 1590, 1570, 1478, 1451 $\nu(\text{Ph/Py})$, 1531 $\delta(\text{N-H})$, 753 $\gamma(\text{C-H})$ cm^{-1} .

Di-*tert*-butyl-1,4,7,10-tetraazacyclododecane-1,7-dicarboxylate (5). This compound was prepared according to the literature.¹⁹ A solution of 1,4,7,10-tetraazacyclododecane (0.714 g, 4.145 mmol) and *tert*-butyl-(oxycarbonyloxy)succinimide (1.820 g, 8.289 mmol) in chloroform (35 mL) was stirred at room temperature for 48 h. The solvent was removed by rotary evaporation and the residue was dissolved in chloroform (30 mL) and washed with an aqueous solution of NaOH 3 M (3 \times 30 mL). The organic layer was combined and dried over anhydrous Na_2SO_4 , and the solvent was evaporated under reduced pressure. The residue was dried under vacuum for several hours to give 1.495 g of the desired compound (84%) as a pale yellow oil. ^1H NMR (500 MHz, CDCl_3 , 298 K): δ 3.33 (m, 8H), 2.81 (m, 8H), 1.41 (s, 18H). ^{13}C NMR (125.8 MHz, CDCl_3 , 298 K): δ 156.3, 156.2, 79.8, 79.6, 50.9, 50.5, 50.3, 50.1, 50.1, 49.4, 48.9, 48.3, 28.6, 28.6. MS-ESI $^+$, m/z (%BPI): [$\mathbf{5} + \text{H}$] $^+$, 373.3 (100%). Elem. Anal. Calcd for $\text{C}_{18}\text{H}_{36}\text{N}_4\text{O}_4\cdot 0.5\text{CHCl}_3$: C, 51.4; H, 8.5; N, 13.0%. Found: C, 52.0; H, 8.5; N, 12.6%. IR: 3010–2827 $\nu(\text{C-H})$, 1682 $\nu(\text{C=O})$, 1157 $\nu_a(\text{N-C})$, 752 $\gamma(\text{C-H})$ cm^{-1} .

Di-*tert*-butyl-4-(2-(3-(3-nitrophenyl)ureido)benzyl)-1,4,7,10-tetraazacyclododecane-1,7-dicarboxylate (6a). A solution of 1-(2-(chloromethyl)phenyl)-3-(3-nitrophenyl)urea (**3a**) (0.283 g, 0.925 mmol) in acetonitrile (50 mL) was added dropwise to a suspension of compound **5** (2.000 g, 4.627 mmol) and potassium carbonate (1.292 g, 9.255 mmol) in acetonitrile (100 mL) and stirred at room temperature for 16 h. The suspension was filtered and the filtrate concentrated to dryness. The residue was extracted with chloroform (5 \times 50 mL) and water (25 mL), the organic layer combined and dried over anhydrous Na_2SO_4 , and the solvent evaporated under reduced pressure. The resulting oil was purified on a CombiFlash RF-200, using a 12 g-silica gel column and $\text{CH}_2\text{Cl}_2/\text{MeOH}$ as eluent (from 0 to 5% of methanol; the desired compound eluted from 1.5 to 3%) to give pure product **6a** as a yellow foam (0.466 g, 74%). ^1H NMR (500 MHz, CDCl_3 , 298 K): δ 9.68 (s), 8.89 (s), 8.42 (m), 7.87–7.80 (m), 7.71 (m), 7.32 (m), 7.24 (m), 6.94 (m), 4.02 (m), 3.65–2.56 (m), 1.36–1.27 (m). ^{13}C NMR (125.8 MHz, CDCl_3 , 298 K): δ 155.3, 153.1, 148.5, 140.9, 138.0, 135.0, 131.5, 129.3, 128.9, 124.9, 124.2, 123.5, 116.6, 113.0, 81.1, 55.3, 53.3, 48.7, 48.2, 47.1, 28.2. MS-ESI $^+$, m/z (%BPI): [$\mathbf{6a} + \text{H}$] $^+$, 642.4 (100%). Elem. Anal. Calcd for $\text{C}_{32}\text{H}_{47}\text{N}_7\text{O}_7\cdot 0.5\text{CH}_2\text{Cl}_2$: C, 57.1; H, 7.1; N, 14.3%. Found: C, 57.1; H, 7.0; N, 13.7%. IR: 3268 $\nu(\text{N-H})$, 3130–2860 $\nu(\text{C-H})$, 1692 $\nu(\text{C=O})$, 1589, 1479, 1452 $\nu(\text{C=C})$, 1526 $\nu_a(\text{NO}_2)$, 1346 $\nu_s(\text{NO}_2)$, 1154 $\nu_a(\text{N-C})$, 749 $\gamma(\text{C-H})$ cm^{-1} .

Di-*tert*-butyl-4-(4-(*tert*-butyl)benzyl)-10-(2-(3-(3-nitrophenyl)ureido)benzyl)-1,4,7,10-tetraazacyclododecane-1,7-dicarboxylate (7a). A solution of 1-(bromomethyl)-4-(*tert*-butyl)benzene (0.186 mL, 0.984 mmol), compound **6a** (0.449 g, 0.656 mmol), *N,N*-diisopropylethylamine (0.231 mL, 1.312 mmol) and a catalytic amount of KI in acetonitrile (50 mL) was heated to reflux with stirring for 16 h. The resulting solution was filtered while hot and the filtrate concentrated to dryness. The residue was extracted with chloroform (5 \times 25 mL) and water (15 mL), the organic layer combined and dried over anhydrous Na_2SO_4 , and the solvent evaporated under reduced pressure. The resulting oil was purified on a CombiFlash RF-200, using a 12 g-silica gel column and Hex/EtOAc as eluent (from 0 to 100% of ethyl acetate; the desired compound eluted from 20 to 50%) to give pure product **7a** as a yellow foam (0.277 g, 54%). ^1H NMR (500 MHz, CDCl_3 , 298 K): δ 9.75 (s), 9.68 (s), 9.47 (s), 9.31 (s), 8.37 (s), 8.31 (s), 8.10 (d, $^3J = 7.9$

Hz), 7.90 (d, $^3J = 7.9$ Hz), 7.78 (ddd, $^3J = 8.2$ Hz, $^4J = 2.2$ Hz, $^4J = 0.8$ Hz), 7.38 (t, $^3J = 8.2$ Hz), 7.34 (d, $^3J = 8.2$ Hz), 7.26 (m), 7.13 (d, $^3J = 7.6$ Hz), 7.10 (m), 6.95 (m), 3.73 (m), 3.34–2.66 (m), 1.48 (s), 1.41 (s), 1.30 (s), 1.19 (s). ^{13}C NMR (125.8 MHz, CDCl_3 , 298 K): δ 157.0, 156.2, 155.7, 153.4, 150.3, 148.5, 141.7, 139.0, 132.0, 130.0, 129.4, 128.2, 127.0, 125.1, 124.6, 122.9, 122.5, 116.3, 113.3, 81.0, 80.1, 79.4, 60.2, 58.9, 56.4, 55.9, 54.9, 53.4, 52.8, 52.6, 50.8, 48.7, 47.8, 45.8, 44.8, 34.5, 31.3, 28.6, 28.5, 28.3. MS-ESI⁺, m/z (%BPI): [**7a** + H]⁺, 788.5 (100%). Elem. Anal. Calcd for $\text{C}_{43}\text{H}_{61}\text{N}_7\text{O}_7$: C, 65.5; H, 7.8; N, 12.4%. Found: C, 65.4; H, 8.0; N, 12.0%. IR: 3320, 3291 $\nu(\text{N-H})$, 2965–2810 $\nu(\text{C-H})$, 1688, 1664 $\nu(\text{C=O})$, 1591, 1479, 1450 $\nu(\text{C=C})$, 1525 $\nu_a(\text{NO}_2)$, 1347 $\nu_s(\text{NO}_2)$, 1151 $\nu_a(\text{N-C})$ cm^{-1} .

1-(2-((7-(4-(tert-Butyl)benzyl)-1,4,7,10-tetraazacyclododecan-1-yl)methyl)phenyl)-3-(3-

nitrophenyl)urea (L**³). A solution of compound **7a** (0.250 g, 0.317 mmol) and trifluoroacetic acid (5 mL) in chloroform (5 mL) was stirred at room temperature for 16 h. The solvent was removed by rotary evaporation and the residue was dissolved in chloroform (30 mL). The acid in excess was neutralised with an aqueous solution of NaOH 1 M and the organic layer washed with distilled water (2 × 15 mL). The organic phase was dried over anhydrous Na_2SO_4 , and the solvent evaporated under reduced pressure to give pure product **L**³ as an orange oil which became a solid after remaining under vacuum for several days (0.179 g, 96%). ^1H NMR (500 MHz, CDCl_3 , 298 K): δ 10.46 (s, 1H), 8.79 (s, 1H), 8.06 (m, 2H, H17 and H27), 7.76 (m, 1H, H23), 7.72 (m, 1H, H25), 7.36–7.28 (m, 2H, H16 and H24), 7.20 (d, 2H, H4, $^3J = 8.2$ Hz), 7.12–7.04 (m, 3H, H5 and H14), 7.00 (td, 1H, H15, $^3J = 7.4$ Hz, $^4J = 1.1$ Hz), 3.65 (s, 2H, H12), 3.49 (s, 2H, H7), 2.93–2.26 (m, H9 and H10), 2.71 (m, H11), 2.57 (m, H8), 1.17 (s, 9H, H1). ^{13}C NMR (125.8 MHz, CDCl_3 , 298 K): δ 153.1 C20, 150.2 C3, 148.5 C26, 141.6 C22, 138.6 C18, 135.4 C6, 130.0 C24, 129.3 C14, 128.7 C16, 128.4 C5, 128.0 C13, 125.3 C4, 124.4 C23, 123.1 C15, 122.5 C17, 116.3 C25, 113.2 C27, 60.8 C12, 59.3 C7, 53.2 C11, 51.1 C8, 46.7 C9, 46.4 C10, 34.4 C2, 31.3 C1. MS-ESI⁺, m/z (%BPI): [**L**³ + H]⁺, 588.4 (100%). Elem. Anal. Calcd for $\text{C}_{33}\text{H}_{45}\text{N}_7\text{O}_3$: C, 67.4; H, 7.7; N, 16.7%. Found: C, 68.0; H, 7.5; N, 16.0%. IR: 3330–3183 $\nu(\text{N-H})$, 2962–2820 $\nu(\text{C-H})$, 1700 $\nu(\text{C=O})$, 1613, 1590, 1483, 1449 $\nu(\text{C=C})$, 1520 $\nu_a(\text{NO}_2)$, 1349 $\nu_s(\text{NO}_2)$ cm^{-1} . Slow evaporation of a solution of the receptor in 1-butanol provided yellow single crystals suitable for X-ray diffraction analysis.**

Di-tert-Butyl-4-(2-(3-(4-hexylphenyl)ureido)benzyl)-1,4,7,10-tetraazacyclododecane-1,7-dicarboxylate

(6b). A solution of compound **3b** (0.319 g, 0.925 mmol) in acetonitrile (50 mL) was added dropwise to a suspension of compound **5** (2.000 g, 4.627 mmol) and potassium carbonate (1.292 g, 9.255 mmol) in acetonitrile (100 mL) and stirred at room temperature for 16 h. The suspension was filtered and the filtrate concentrated to dryness. The residue was extracted with chloroform (5 × 50 mL) and water (25 mL), the organic layer combined and dried over anhydrous Na_2SO_4 , and the solvent evaporated under reduced pressure. The resulting oil was purified on a CombiFlash RF-200, using a 12 g-silica gel column and $\text{CH}_2\text{Cl}_2/\text{MeOH}$ as eluent (from 0 to 5% of methanol; the desired compound eluted from 1.5 to 3%) to give pure product **6b** as a white foam (0.436 g, 69%). ^1H NMR (500 MHz, CDCl_3 , 298 K): δ 12.10 (s), 11.35 (s), 9.72 (s), 9.52 (s), 9.18 (s), 9.04 (s), 8.87 (s), 7.95–7.88 (m), 7.48 (d, $^3J = 8.0$ Hz), 7.32 (m), 7.07 (d, $^3J = 8.4$ Hz), 7.03–6.97 (m), 4.28 (m), 4.15 (s), 3.97 (m), 3.69–2.64 (m), 2.53 (m), 1.57 (m), 1.44–1.42 (m), 1.29 (m), 0.87 (m). ^{13}C NMR (125.8 MHz, CDCl_3 , 298 K): δ 155.6, 155.4, 154.3, 154.0, 138.6, 137.2, 137.0, 131.6, 131.5, 129.3, 128.8, 125.5, 123.6, 119.1, 81.8, 81.6, 81.4, 55.9, 53.9, 50.0, 48.9, 48.8, 48.4, 48.1, 47.4, 35.5, 31.9, 31.7, 29.1, 28.5, 22.8, 14.2. MS-ESI⁺, m/z (%BPI): [**6b** + H]⁺, 681.5 (100%). Elem. Anal. Calcd for $\text{C}_{38}\text{H}_{60}\text{N}_6\text{O}_5$: C, 67.0; H, 8.9; N, 12.3%. Found: C, 66.7; H, 8.9; N, 12.0%. IR: 3271 $\nu(\text{N-H})$, 3120–2855 $\nu(\text{C-H})$, 1693 $\nu(\text{C=O})$, 1605, 1588, 1478, 1453 $\nu(\text{C=C})$, 1538 $\delta(\text{N-H})$, 1155 $\nu_a(\text{N-C})$, 751 $\gamma(\text{C-H})$ cm^{-1} .

Di-tert-Butyl-4-(4-(tert-butyl)benzyl)-10-(2-(3-(4-hexylphenyl)ureido)benzyl)-1,4,7,10-

tetraazacyclododecane-1,7-dicarboxylate (7b). A solution of 1-(bromomethyl)-4-(tert-butyl)benzene (0.179 mL, 0.946 mmol), compound **6b** (0.429 g, 0.630 mmol), *N,N*-diisopropylethylamine (0.222 mL, 1.261 mmol) and a catalytic amount of KI in acetonitrile (50 mL) was heated to reflux with stirring for 16 h. The resulting solution was filtered while hot and the filtrate concentrated to dryness. The residue was extracted

with chloroform (5 × 25 mL) and water (15 mL), the organic layer combined and dried over anhydrous Na₂SO₄, and the solvent evaporated under reduced pressure. The resulting oil was purified on a CombiFlash RF-200, using a 12 g-silica gel column and Hex/EtOAc as eluent (from 0 to 100% of ethyl acetate; the desired compound eluted from 20 to 50%) to give pure product **7b** as a pale brown foam (0.275 g, 53%). ¹H NMR (500 MHz, CDCl₃, 298 K): δ 9.35 (s), 8.87 (s), 8.78 (s), 7.89 (d, ³J = 8.0 Hz), 7.48 (d, ³J = 7.8 Hz), 7.35 (d, ³J = 8.2 Hz), 7.31 (m), 7.26 (m), 7.21 (m), 7.17–7.13 (m), 7.07 (d, ³J = 8.4 Hz), 6.93 (m), 3.72 (m), 3.59–2.65 (m), 2.54 (m), 1.58 (m), 1.48–1.40 (m), 1.31 (s), 1.30 (m), 1.22 (s), 0.88 (m). ¹³C NMR (125.8 MHz, CDCl₃, 298 K): δ 156.9, 156.0, 154.1, 150.5, 149.8, 139.8, 137.9, 136.6, 135.3, 132.3, 130.1, 128.7, 128.3, 127.2, 125.3, 125.2, 125.1, 122.9, 122.5, 119.2, 80.8, 80.1, 79.6, 60.4, 56.7, 56.3, 55.1, 53.5, 52.8, 51.2, 48.8, 47.9, 46.0, 45.2, 35.5, 34.6, 31.9, 31.8, 31.5, 31.5, 29.1, 28.7, 28.6, 28.5, 22.8, 14.3. MS-ESI⁺, *m/z* (%BPI): [**7b** + H]⁺, 827.6 (100%). Elem. Anal. Calcd for C₄₉H₇₄N₆O₅: C, 71.2; H, 9.0; N, 10.2%. Found: C, 71.5; H, 8.9; N, 9.4%. IR: 3336 ν(N–H), 2961–2800 ν(C–H), 1688, 1672 ν(C=O), 1590, 1477, 1451 ν(C=C), 1529 δ(N–H), 1151 ν_a(N–C) cm⁻¹.

1-(2-((7-(4-(*tert*-Butyl)benzyl)-1,4,7,10-tetraazacyclododecan-1-yl)methyl)phenyl)-3-(4-

hexylphenyl)urea (L⁴). A solution of compound **7b** (0.236 g, 0.285 mmol) and trifluoroacetic acid (5 mL) in chloroform (5 mL) was stirred at room temperature for 16 h. The solvent was removed by rotary evaporation and the residue was dissolved in chloroform (30 mL). The acid in excess was neutralized with an aqueous solution of NaOH 1 M and the organic layer washed with distilled water (2 × 15 mL). The organic phase was dried over anhydrous Na₂SO₄, and the solvent evaporated under reduced pressure to give pure product **L⁴** as a brown oil which became a solid after remaining under vacuum for several days (0.178 g, 100%). ¹H NMR (500 MHz, CDCl₃, 298 K): δ 9.63 (s, 1H, H21), 8.21 (s, 1H, H19), 8.06 (m, 1H, H17), 7.51 (d, 2H, H23, ³J = 8.5 Hz), 7.27 (m, H16), 7.21 (d, 2H, H4, ³J = 8.3 Hz), 7.06 (m, 1H, H14), 7.01 (d, 2H, H24, ³J = 8.5 Hz), 6.95 (m, 1H, H15), 6.89 (d, 2H, H5, ³J = 8.2 Hz), 3.71 (s, 2H, H12), 3.45 (s, 2H, H7), 2.61 (s, H11), 2.53–2.34 (m, H8, H9 and H10), 1.49 (m, 2H, H27), 1.26 (m, H1, H28, H29 and H30), 0.86 (m, 3H, H31). ¹³C NMR (125.8 MHz, CDCl₃, 298 K): δ 154.5 C20, 150.3 C3, 138.9 C18, 137.6 C22, 136.9 C25, 134.5 C6, 131.4 C14, 128.8 C16, 128.8 C24, 128.7 C5, 127.3 C13, 125.3 C4, 122.9 C15, 122.8 C17, 118.9 C23, 61.3 C12, 59.5 C7, 52.3 C11, 50.5 C8 and C9, 47.5 C10, 35.3 C26, 34.5 C2, 31.8 C27, 31.8 C28, 31.4 C1, 29.1 C29, 22.7 C30, 14.2 C31. MS-ESI⁺, *m/z* (%BPI): [**L⁴** + H]⁺, 627.5 (100%). Elem. Anal. Calcd for C₃₉H₅₈N₆O: C, 74.7; H, 9.3; N, 13.4%. Found: C, 75.3; H, 9.3; N, 13.2%. IR: 3320–3187 ν(N–H), 3120–2819 ν(C–H), 1702 ν(C=O), 1611, 1588, 1448 ν(C=C), 749 γ(C–H) cm⁻¹.

General procedure for the preparation of [ML³Cl₂], [ML³(SO₄)] and [ML³(NO₃)₂] (M = Cu or Zn)

A solution of MCl₂ or hydrated M(NO₃)₂ or M(SO₄) (0.085 mmol, M = Cu or Zn) in methanol (2 mL) was added to a solution of **L³** (0.050 g, 0.085 mmol) in methanol (5 mL). The mixture was stirred at room temperature for 16 h, and the precipitate formed was isolated by filtration, washed with methanol (2 mL) and diethyl ether (2 mL) and dried under vacuum. In some cases an additional purification step was required to remove metal salt impurities: the solvent was evaporated under reduced pressure and the precipitate dissolved in chloroform (5 mL); the solution was then filtered and the filtrate concentrated to dryness. The solid was treated with diethyl ether (5 mL), filtrated and dried under vacuum.

[CuL³Cl₂]·3MeOH. Dark green solid. Yield: 0.050 g, 71%. MS-ESI⁺, *m/z* (%BPI): [Cu(L³)Cl]⁺, 685.3 (15%); [Cu(L³ – H)]⁺, 649.3 (100%); [Cu(L³)]²⁺, 325.2 (10%). Elem. Anal. Calcd for C₃₃H₄₅Cl₂CuN₇O₃·3MeOH: C, 52.8; H, 7.0; N, 12.0%. Found: C, 52.9; H, 6.5; N, 11.6%. *A_M* (MeOH, 10⁻³ M, 25 °C): 89.1 cm² Ω⁻¹ mol⁻¹ (1 : 1 electrolyte). IR: 3187 ν(N–H), 3120–2870 ν(C–H), 1695 ν(C=O), 1588ν(C=C), 1524 ν_a(NO₂), 1345 ν_s(NO₂), 736 γ(C–H) cm⁻¹. UV/vis diffuse reflectance spectroscopy: 678 nm.

[CuL³(NO₃)₂]·0.5CHCl₃·2MeOH. Dark blue solid. Yield: 0.045 g, 59%. Elem. Anal. Calcd for C₃₃H₄₅CuN₉O₉·0.5CHCl₃·2MeOH: C, 47.4; H, 6.0; N, 14.0%. Found: C, 47.7; H, 6.1; N, 13.6. *A_M* (MeOH,

10^{-3} M, 25 °C): $173.1 \text{ cm}^2 \Omega^{-1} \text{ mol}^{-1}$ (2 : 1 electrolyte). IR: $3230 \nu(\text{N-H})$, $3120\text{--}2870 \nu(\text{C-H})$, $1714 \nu(\text{C=O})$, $1526 \nu_a(\text{NO}_2)$, $1317 \nu_a(\text{N-O})$, $735 \delta_a(\text{O-N-O}) \text{ cm}^{-1}$. UV/vis diffuse reflectance spectroscopy: 594 nm.

[CuL³(SO₄)·1.5H₂O]. Light blue solid. Yield: 0.039 g, 59%. MS-ESI⁺, *m/z* (%BPI): [Cu(L³ - H)]⁺, 649.3 (100%); [Cu(L³)]²⁺, 325.2 (33%). Elem. Anal. Calcd for C₃₃H₄₅CuN₇O₇S·1.5H₂O: C, 51.2; H, 6.3; N, 12.7%. Found: C, 51.1; H, 6.2; N, 12.5%. *A_M* (MeOH, 10⁻³ M, 25 °C): $7.8 \text{ cm}^2 \Omega^{-1} \text{ mol}^{-1}$ (non-electrolyte). IR: $3223 \nu(\text{N-H})$, $3130\text{--}2870 \nu(\text{C-H})$, $1711 \nu(\text{C=O})$, $1589 \nu(\text{C=C})$, $1545 \delta(\text{N-H})$, $1525 \nu_a(\text{NO}_2)$, $1350 \nu_s(\text{NO}_2)$, 1106 , 1088 , $1026 \nu_a(\text{S-O})$, $739 \gamma(\text{C-H})$, 616 , $597 \delta_a(\text{O-S-O}) \text{ cm}^{-1}$. UV/vis diffuse reflectance spectroscopy: 657 nm. Slow evaporation of a solution of the complex in a chloroform/methanol mixture provided dark blue single crystals suitable for X-ray diffraction analysis.

[CuL³(ClO₄)₂]·2H₂O. Dark green solid. Yield: 0.067 g, 88%. MS-ESI⁺, *m/z* (%BPI): [Cu(L³)]⁺, 649.3 (1%). Elem. Anal. Calcd for C₃₃H₄₅Cl₂CuN₇O₁₁·2H₂O: C, 44.7; H, 5.6; N, 11.1%. Found: C, 44.4; H, 4.5; N, 10.9%. *A_M* (MeOH, 10⁻³ M, 25 °C): $163 \text{ cm}^2 \Omega^{-1} \text{ mol}^{-1}$ (2 : 1 electrolyte). IR: 3354 , $3279 \nu(\text{N-H})$, $3090\text{--}2860 \nu(\text{C-H})$, $1529 \nu_a(\text{NO}_2)$, $1349 \nu_s(\text{NO}_2)$, $1076 \nu_a(\text{Cl-O})$, $621 \delta_a(\text{O-Cl-O}) \text{ cm}^{-1}$. UV/vis diffuse reflectance spectroscopy: 589 nm.

[ZnL³Cl₂]·2MeOH. Light brown solid. Yield: 0.053 g, 79%. MS-ESI⁺, *m/z* (%BPI): [Zn(L³ - H)]⁺, 650.3 (100%). Elem. Anal. Calcd for C₃₃H₄₅Cl₂N₇O₃Zn·2MeOH: C, 53.3; H, 6.8; N, 12.4%. Found: C, 53.3; H, 6.5; N, 12.2%. *A_M* (MeOH, 10⁻³ M, 25 °C): $76.6 \text{ cm}^2 \Omega^{-1} \text{ mol}^{-1}$ (1 : 1 electrolyte). IR: $3227 \nu(\text{N-H})$, $3130\text{--}2875 \nu(\text{C-H})$, $1697 \nu(\text{C=O})$, 1605 , $1588 \nu(\text{C=C})$, $1524 \nu_a(\text{NO}_2)$, $1345 \nu_s(\text{NO}_2)$, $737 \gamma(\text{C-H}) \text{ cm}^{-1}$. ¹H NMR (500 MHz, dms_o-*d*₆, 298 K): δ 10.12 (s), 9.70 (s), 9.11 (s), 8.97 (s), 8.61 (s), 8.57 (s), 7.83–7.76 (m), 7.58 (m), 7.44–7.37 (m), 7.30–7.19 (m), 4.77 (s), 3.98 (s), 3.88 (s), 3.83 (s), 3.73 (s), 3.15 (s), 2.98 (m), 2.76–2.65 (m), 1.27 (s). ¹³C NMR (125.8 MHz, dms_o-*d*₆, 298 K): δ 153.6, 150.6, 149.9, 148.2, 141.5, 141.4, 137.9, 137.3, 132.7, 131.9, 131.1, 130.9, 130.1, 129.8, 129.7, 129.5, 129.3, 129.2, 129.0, 128.4, 128.1, 127.9, 127.4, 126.3, 126.0, 125.3, 125.2, 124.9, 124.3, 124.1, 116.2, 116.1, 112.1, 112.0, 55.9, 55.5, 51.5, 51.3, 48.7, 47.1, 46.8, 42.9, 42.9, 42.6, 42.5, 34.3, 34.3, 31.2, 31.1.

[ZnL³(NO₃)₂]·CHCl₃. Light brown solid. Yield: 0.064 g, 84%. MS-ESI⁺, *m/z* (%BPI): [Zn(L³ - H)]⁺, 650.3 (100%). Elem. Anal. Calcd for C₃₃H₄₅N₉O₉Zn·CHCl₃: C, 45.6; H, 5.2; N, 14.1%. Found: C, 45.8; H, 5.3; N, 13.4. *A_M* (MeOH, 10⁻³ M, 25 °C): $133.5 \text{ cm}^2 \Omega^{-1} \text{ mol}^{-1}$. IR: $3251 \nu(\text{N-H})$, $3120\text{--}2860 \nu(\text{C-H})$, $1695 \nu(\text{C=O})$, $1601 \nu(\text{C=C})$, $1525 \nu_a(\text{NO}_2)$, 1343 , 1323 , $1293 \nu_a(\text{N-O})$, $737 \delta_a(\text{O-N-O}) \text{ cm}^{-1}$. ¹H NMR (500 MHz, dms_o-*d*₆, 298 K): δ 9.70 (s), 9.59 (s), 8.79 (s), 8.77 (s), 8.60 (m), 8.57 (m), 7.82 (m), 7.75 (m), 7.57 (m), 7.45–7.37 (m), 7.29–7.21 (m), 4.77 (s), 3.97 (s), 3.84 (s), 3.81 (s), 3.73 (s), 3.16 (s), 3.04 (m), 2.75 (m), 2.56 (m), 1.27 (s). ¹³C NMR (125.8 MHz, dms_o-*d*₆, 298 K): δ 153.6, 153.6, 150.8, 150.0, 148.2, 141.4, 141.4, 137.9, 137.1, 132.6, 132.0, 131.0, 130.2, 130.1, 129.9, 129.6, 129.2, 129.0, 128.5, 128.1, 127.7, 127.5, 126.6, 126.1, 125.5, 125.3, 125.2, 124.6, 124.4, 124.3, 116.3, 116.3, 112.2, 112.1, 55.6, 55.2, 51.2, 50.7, 48.9, 47.1, 46.8, 42.8, 42.8, 42.6, 42.5, 34.4, 34.3, 31.2, 31.2. Slow diffusion of diethyl ether into a solution of the complex in an acetonitrile/methanol mixture gave pale yellow single crystals suitable for X-ray diffraction analysis.

[ZnL³(SO₄)]. Light yellow solid. Yield: 0.042 g, 66%. MS-ESI⁺, *m/z* (%BPI): [Zn(L³ - H)]⁺, 650.3 (100%). Elem. Anal. Calcd for C₃₃H₄₅N₇O₇SZn: C, 52.9; H, 6.1; N, 13.1%. Found: C, 52.6; H, 6.0; N, 12.9%. *A_M* (MeOH, 10⁻³ M, 25 °C): the low solubility of this complex in methanol has prevented us from determining the conductivity value for this compound. IR: $3228 \nu(\text{N-H})$, $3130\text{--}2882 \nu(\text{C-H})$, $1712 \nu(\text{C=O})$, $1590 \nu(\text{C=C})$, $1550 \delta(\text{N-H})$, $1529 \nu_a(\text{NO}_2)$, $1348 \nu_s(\text{NO}_2)$, $1024 \nu_a(\text{S-O})$, 611 , $593 \delta_a(\text{O-S-O}) \text{ cm}^{-1}$. δ_{H} and δ_{C} (solvent dms_o-*d*₆): the low solubility of this complex in dms_o-*d*₆ has prevented us from recording its ¹H and ¹³C NMR spectra.

[ZnL³(ClO₄)₂]·H₂O. Light brown solid. Yield: 0.065 g, 88%. MS-ESI⁺, *m/z* (%BPI): [Zn(L³ - H)]⁺, 650.3 (100%). Elem. Anal. Calcd for C₃₃H₄₅Cl₂N₇O₁₁Zn·H₂O: C, 45.6; H, 5.4; N, 11.3%. Found: C, 45.4; H, 4.9; N, 11.2%. *A_M* (MeOH, 10⁻³ M, 25 °C): $186.8 \text{ cm}^2 \Omega^{-1} \text{ mol}^{-1}$ (2 : 1 electrolyte). IR: $3361\text{--}3288 \nu(\text{N-H})$,

3090–2870 $\nu(\text{C-H})$, 1528 $\nu_a(\text{NO}_2)$, 1348 $\nu_s(\text{NO}_2)$, 1069 $\nu_a(\text{Cl-O})$, 621 $\delta_a(\text{O-Cl-O}) \text{ cm}^{-1}$. $^1\text{H NMR}$ (500 MHz, $\text{dms}\text{-}d_6$, 298 K): δ 9.38 (s), 8.56 (m), 8.54 (m), 8.16 (s), 7.87 (m), 7.84 (m), 7.75 (m), 7.66 (m), 7.58 (m), 7.42 (m), 7.33 (m), 7.26 (m), 7.02 (m), 4.77 (s), 3.98 (s), 3.85 (s), 3.04 (s), 2.86 (s), 2.72 (m), 1.28 (m). $^{13}\text{C NMR}$ (125.8 MHz, $\text{dms}\text{-}d_6$, 298 K): δ 157.0, 153.7, 150.9, 150.7, 148.2, 147.9, 146.8, 143.4, 141.3, 137.8, 132.7, 132.5, 131.0, 130.9, 130.2, 130.1, 129.6, 129.4, 129.3, 129.0, 127.9, 127.4, 126.1, 126.0, 125.6, 125.4, 125.3, 125.0, 124.5, 122.2, 116.5, 114.9, 112.8, 112.3, 56.0, 55.7, 55.3, 50.9, 48.9, 48.8, 42.8, 42.7, 34.4, 31.2, 31.2.

Solvent extraction experiments

Inductively coupled plasma optical emission spectroscopy (ICP-OES) analysis was performed on a Perkin Elmer Optima 5300DV spectrometer and standards were purchased from Alfa Aesar. Organic ICP-OES samples were made up by evaporating 1 mL samples of the organic phase and re-dissolving in 10 mL butan-1-ol. The measurements of pH were carried out using a Sartorius PP-50 pH meter. All extractions were performed by vigorously stirring solutions with magnetic stirring bars in sealed 20 mL vials for 16 h at room temperature (see solvent extraction details for different experiments, ESI†).

Table 4. Crystal data and refinement details for L^3 , $[\text{CuL}^3(\text{SO}_4)] \cdot \text{MeOH}$, $[\text{ZnL}^3(\text{NO}_3)](\text{NO}_3) \cdot 0.75\text{MeOH}$ and $[\text{CuL}^1(\mu\text{-SO}_4)]_2 \cdot \text{C}_6\text{H}_6\text{N}_2\text{O}_2$

	L^3	$[\text{CuL}^3(\text{SO}_4)] \cdot \text{MeOH}$	$[\text{ZnL}^3(\text{NO}_3)](\text{NO}_3) \cdot 0.75\text{MeOH}$	$[\text{CuL}^1(\mu\text{-SO}_4)]_2 \cdot \text{C}_6\text{H}_6\text{N}_2\text{O}_2$
Formula	$\text{C}_{33}\text{H}_{45}\text{N}_7\text{O}_3$	$\text{C}_{34}\text{H}_{49}\text{CuN}_7\text{O}_8\text{S}$	$\text{C}_{33.75}\text{H}_{49}\text{N}_9\text{O}_{9.75}\text{Zn}$	$\text{C}_{64}\text{H}_{60}\text{Cu}_2\text{N}_{16}\text{O}_{18}\text{S}_2$
MW	587.76	779.40	801.18	1532.48
Crystal system	Monoclinic	Triclinic	Monoclinic	Triclinic
Space group	$P2_1/c$	$P\bar{1}$	$C2/c$	$P\bar{1}$
T/K	100(2)	100(2)	100(2)	100(2)
$a/\text{\AA}$	14.901(1)	10.1147(4)	37.519(1)	8.9322(4)
$b/\text{\AA}$	11.9675(8)	10.8086(4)	10.8462(3)	13.2792(6)
$c/\text{\AA}$	17.987(1)	16.8713(7)	22.2476(7)	14.2039(6)
$\alpha/^\circ$	90	76.478(2)	90	86.497(2)
$\beta/^\circ$	92.980(5)	78.801(2)	122.529(2)	88.233(2)
$\gamma/^\circ$	90	79.307(2)	90	72.795(2)
$V/\text{\AA}^3$	3203.1(4)	1740.1(1)	7633.1(4)	1606.2(1)
$F(000)$	1264	822	3372	790
Z	4	2	8	1
$\lambda, \text{\AA} (\text{MoK}\alpha)$	0.71073	0.71073	0.71073	0.71073
$D_{\text{calc}}/\text{g cm}^{-3}$	1.219	1.488	1.394	1.584
μ/mm^{-1}	0.080	0.751	0.710	0.815
θ range/ $^\circ$	2.04–28.33	2.07–28.45	1.99–28.38	2.45–26.52
R_{int}	0.0672	0.0477	0.0802	0.0361
Reflections measured	56 699	35 120	65 309	27 518
Unique reflections	7961	8657	9555	6573
Reflections observed	5521	7031	6540	5552
GOF on F^2	1.033	1.030	1.048	1.047
R_1^a	0.0483	0.0385	0.0542	0.0304
wR_2^b	0.1231	0.1036	0.1637	0.0765
Largest diff. peak & hole/ \AA^{-3}	0.382 and -0.258	0.886 and -0.538	1.435 and -0.746	0.408 and -0.406
CCDC deposition number	1525437	1525438	1525435	1525436

^a $R_1 = \sum ||F_o| - |F_c|| / \sum |F_o|$. ^b $wR_2 (\text{all data}) = \{ \sum [w(|F_o|^2 - |F_c|^2)^2] / \sum [w(F_o^4)] \}^{1/2}$.

X-ray diffraction studies

Single crystals were obtained from solutions of the isolated compounds, as described above. Three dimensional X-ray data were collected on a BRUKER-NONIUS X8 APEX KAPPA CCD diffractometer. Data were corrected for Lorentz and polarisation effects and for absorption by semiempirical methods⁴⁹ based on symmetry-equivalent reflections. Complex scattering factors were taken from the SHELXL (version 2014/7 or 2016/6 only for the Zn complex) programs⁵⁰ running under the WinGX program system⁵¹ as implemented on a Pentium computer. The structures were solved either by Patterson methods with DIRDIF2008,⁵² except that of **L**³, which was solved by direct methods using the SHELXL programs.⁵⁰ All structures were refined by full-matrix least-squares on F^2 . For the four compounds all hydrogen atoms were included in calculated positions and refined in riding mode, except some hydrogen atoms involved in hydrogen bonding that were refined freely (H2N, H3N, H5N H6N in **L**³; H3N in [Cu**L**³(SO₄)]·MeOH and H2A, H2B, H3N, H5N and H6N in [Zn**L**³(NO₃)](NO₃)·0.75MeOH and H2N and H3N in [Cu**L**¹(μ-SO₄)₂·C₆H₆N₂O₂). The crystal structure of [Cu**L**³(SO₄)]·MeOH shows positional disorder for the sulfate anion with an occupation factor of 0.77(2) for the atoms labelled as A. The crystal of [Zn**L**³(NO₃)](NO₃)·0.75MeOH also shows positional disorder affecting one of the nitrate anions, the *tert*-butyl group and the distal part of the urea moiety. The occupancy factors for the positions labelled as A for the nitrate anion were 0.574(6) and 0.60(2) for the *tert*-butyl group. The methanol molecules show occupancy factors of 0.430(4) (1S) and 0.320(4) (2S). 182 least-squares restraints had to be imposed to reach convergence. Refinement converged with anisotropic displacement parameters for all non-hydrogen atoms for all four crystals. Crystal data and details on data collection and refinement are summarised in Table 4.

CCDC [1525435–1525438](#) contain the supplementary crystallographic data for this paper.

Acknowledgments

The authors thank Xunta de Galicia (EM 2012/088) and (CN-2012/011) for generous financial support and Centro de Supercomputación de Galicia (CESGA) for providing the computer facilities. I. C.-B. thanks Ministerio de Educación y Ciencia (FPU program) for a predoctoral fellowship.

Notes and references

1. (a) J. R. Turkington, P. J. Bailey, J. B. Love, A. M. Wilson and P. A. Tasker, *Chem. Commun.*, 2013, **49**, 1891; (b) A. M. Wilson, P. J. Bailey, P. A. Tasker, J. R. Turkington, R. A. Grant and J. B. Love, *Chem. Soc. Rev.*, 2014, **43**, 123; (c) J. Szymanowski, *Hydroxyoximes and Copper Hydrometallurgy*, CRC Press, 1990.
2. M. Cox, in *Solvent Extraction Principles and Practice*, ed. J. Rydberg, M. Cox, C. Musikas and G. R. Choppin, Marcel Dekker, Inc, New York, 2nd edn, 2004, ch. 11.
3. D. S. Flett, *J. Organomet. Chem.*, 2005, **690**, 2426.
4. M. K. Jha, V. Kumar and R. J. Singh, *Solvent Extr. Ion Exch.*, 2002, **20**, 389.
5. *Comprehensive Coordination Chemistry II*, ed. P. A. Tasker, P. G. Plieger and L. C. West, Elsevier Ltd., Oxford, 2004.
6. Y. Marcus, *Ion Properties*, Marcel Dekker, New York, 1997.

7. C. J. Fowler, T. J. Haverlock, B. A. Moyer, J. A. Shriver, D. E. Gross, M. Marquez, J. L. Sessler, M. A. Hossain and K. Bowman-James, *J. Am. Chem. Soc.*, 2008, **130**, 14386.
8. (a) J. M. Mahoney, K. A. Stucker, H. Jiang, I. Carmichael, N. R. Brinkmann, A. M. Beatty, B. C. Noll and B. D. Smith, *J. Am. Chem. Soc.*, 2005, **127**, 2922; (b) R. J. Ellis, J. Chartres, P. A. Tasker and K. C. Sole, *Solvent Extr. Ion Exch.*, 2011, **29**, 657.
9. (a) T. Lin, V. Gasperov, K. J. Smith, C. C. Tong and P. A. Tasker, *Dalton Trans.*, 2010, **39**, 9760; (b) G. W. Bates, J. E. Davidson, R. S. Forgan, P. A. Gale, D. K. Henderson, M. G. King, M. E. Light, S. J. Moore, P. A. Tasker and C. C. Tong, *Supramol. Chem.*, 2012, **24**, 117.
10. (a) L. Tjioe, A. Meininger, T. Joshi, L. Spiccia and B. Graham, *Inorg. Chem.*, 2011, **50**, 4327; (b) L. Tjioe, T. Joshi, C. M. Forsyth, B. Moubaraki, K. S. Murray, J. Brugger, B. Graham and L. Spiccia, *Inorg. Chem.*, 2012, **51**, 939.
11. (a) T. Guchhait, B. Barua, A. Biswas, B. Basak and G. Mani, *Dalton Trans.*, 2015, **44**, 9091; (b) I.-W. Park, J. Yoo, S. Adhikari, J. S. Park, J. L. Sessler and C.-H. Lee, *Chem. – Eur. J.*, 2012, **18**, 15073; (c) I.-W. Park, J. Yoo, B. Kim, S. Adhikari, S. K. Kim, Y. Yeon, C. J. E. Haynes, J. L. Sutton, C. C. Tong, V. M. Lynch, J. L. Sessler, P. A. Gale and C.-H. Lee, *Chem. – Eur. J.*, 2012, **18**, 2514.
12. (a) T. K. Ghosh, R. Dutta and P. Ghosh, *Inorg. Chem.*, 2016, **55**, 3640; (b) M. Yamamura, J. Miyake, Y. Imamura and T. Nabeshima, *Chem. Commun.*, 2011, **47**, 6801.
13. V. Amendola, D. Esteban-Gómez, L. Fabrizzi, M. Licchelli, E. Monzani and F. Sancenon, *Inorg. Chem.*, 2005, **44**, 8690.
14. I. Carreira-Barral, T. Rodríguez-Blas, C. Platas-Iglesias, A. de Blas and D. Esteban-Gómez, *Inorg. Chem.*, 2014, **53**, 2554.
15. L. M. P. Lima, D. Esteban-Gómez, R. Delgado, C. Platas-Iglesias and R. Tripier, *Inorg. Chem.*, 2012, **51**, 6916.
16. R. D. Hancock, M. S. Shaikjee, S. M. Dobson and J. C. A. Boeyens, *Inorg. Chim. Acta*, 1988, **154**, 229.
17. G. Anderegg, E. Hubmann, N. G. Podder and F. Wenk, *Helv. Chim. Acta*, 1977, **60**, 123.
18. (a) C. V. Esteves, P. Lamosa, R. Delgado, J. Costa, P. Desorege, Y. Rousselin, C. Goze and F. Denat, *Inorg. Chem.*, 2013, **52**, 5138; (b) L. M. P. Lima, C. V. Esteves, R. Delgado, P. Hermann, J. Kotek, R. Sevcikova and P. Lubal, *Eur. J. Inorg. Chem.*, 2012, 2533.
19. J. M. De León-Rodríguez, Z. Kovacs, A. C. Esqueda-Oliva and A. D. Miranda-Olvera, *Tetrahedron Lett.*, 2006, **47**, 6937.
20. (a) M. Woods, S. Aime, M. Botta, J. A. K. Howard, J. M. Moloney, M. Navet, D. Parker, M. Port and O. Rousseaux, *J. Am. Chem. Soc.*, 2000, **122**, 9781; (b) S. Aime, A. Barge, J. I. Bruce, M. Botta, J. A. K. Howard, J. M. Moloney, D. Parker, A. S. De Sousa and M. Woods, *J. Am. Chem. Soc.*, 1999, **121**, 5762; (c) A. Rodríguez-Rodríguez, Z. Garda, E. Ruscsak, D. Esteban-Gomez, A. de Blas, T. Rodríguez-Blas, L. M. P. Lima, M. Beyler, R. Tripier, G. Tircso and C. Platas-Iglesias, *Dalton Trans.*, 2015, **44**, 5017.

21. (a) R. Martínez-Máñez and F. Sacenon, *Chem. Rev.*, 2003, **103**, 4419; (b) M. Regueiro-Figueroa, K. Djanashvili, D. Esteban-Gómez, A. de Blas, C. Platas-Iglesias and T. Rodríguez-Blas, *Eur. J. Org. Chem.*, 2010, 3237.
22. (a) B. J. Hathaway, *Struct. Bonding*, 1973, **14**, 49; (b) A. W. Addison, T. Nageswara-Rao, J. Reedijk, J. van Rijn and G. C. Verschoor, *J. Chem. Soc., Dalton Trans.*, 1984, 1349.
23. (a) A. Carné-Sánchez, C. S. Bonnet, I. Imaz, J. Lorenzo, E. Tóth and D. MasPOCH, *J. Am. Chem. Soc.*, 2013, **135**, 1771 ; (b) Y. Habata, M. Ikeda, A. K. Sah, K. Noto and S. Kuwahara, *Inorg. Chem.*, 2013, **52**, 11697; (c) C. V. Esteves, J. Madureira, L. M. P. Lima, P. Mateus, I. Bento and R. Delgado, *Inorg. Chem.*, 2014, **53**, 4371.
24. (a) J. K. Beattie, *Acc. Chem. Res.*, 1971, **4**, 253; (b) L. M. P. Lima, D. Esteban-Gómez, R. Delgado, C. Platas-Iglesias and R. Tripier, *Inorg. Chem.*, 2012, **51**, 6916.
25. (a) Z. Vargová, R. Gyepes, L. Arabuli, K. Györyová, P. Hermann and I. Lukes, *Inorg. Chim. Acta*, 2009, **362**, 3860; (b) M. H. Salter, J. H. Reibenspies, S. B. Jones and R. D. Hancock, *Inorg. Chem.*, 2005, **44**, 2791; (c) M. Subat, A. S. Borovik and B. König, *J. Am. Chem. Soc.*, 2004, **126**, 3185; (d) E. Kimura, N. Katsube, T. Koike, M. Shiro and S. Aoki, *Supramol. Chem.*, 2002, **14**, 95; (e) T. Koike, T. Watanabe, S. Aoki, E. Kimura and M. Shiro, *J. Am. Chem. Soc.*, 1996, **118**, 12696; (f) A. Schrod, A. Neubrand and R. van Eldik, *Inorg. Chem.*, 1997, **36**, 4579; (g) E. Kimura, T. Ikeda, M. Shionoya and M. Shiro, *Angew. Chem., Int. Ed. Engl.*, 1995, **34**, 663.
26. B. P. Hay, M. Gutowski, D. A. Dixon, J. Garza, R. Vargas and B. A. Moyer, *J. Am. Chem. Soc.*, 2004, **126**, 7925.
27. L.-J. Yang, T. Lei, W. Liu, W.-Q. Chen, M.-S. Lin, L. Li, W. Li and Y. Li, *Inorg. Chem. Commun.*, 2012, **21**, 12.
28. T. K. Ghosh, R. Dutta and P. Ghosh, *Inorg. Chem.*, 2016, **55**, 3640.
29. B. P. Hay, D. A. Dixon, J. C. Bryan and B. A. Moyer, *J. Am. Chem. Soc.*, 2002, **124**, 182.
30. (a) J. M. Tao, J. P. Perdew, V. N. Staroverov and G. E. Scuseria, *Phys. Rev. Lett.*, 2003, **91**, 146401; (b) A. Schaefer, H. Horn and R. Ahlrichs, *J. Chem. Phys.*, 1992, **97**, 2571.
31. J. Tomasi, B. Mennucci and R. Cammi, *Chem. Rev.*, 2005, **105**, 2999.
32. (a) M. Sarma, T. Chatterjee and S. K. Das, *Inorg. Chem. Commun.*, 2010, **13**, 1114; (b) F. C. Fredrick and K. E. Johnson, *J. Inorg. Nucl. Chem.*, 1981, **43**, 1483.
33. G. Ambrosi, M. Formica, V. Fusi, L. Giorgi, A. Guerri, M. Micheloni, P. Paoli, R. Pontellini and P. Rossi, *Chem. – Eur. J.*, 2007, **13**, 702.
34. D. Esteban-Gómez, L. Fabbrizzi, M. Licchelli and E. Monzani, *Org. Biomol. Chem.*, 2005, **3**, 1495.
35. M. Boiocchi, L. Del Boca, D. Esteban-Gómez, L. Fabbrizzi, M. Licchelli and E. Monzani, *Chem. – Eur. J.*, 2005, **11**, 3097.
36. G. Jakab, C. Tancon, Z. Zhang, K.-M. Lippert and P. R. Schreiner, *Org. Lett.*, 2012, **14**, 1724.
37. M. Boiocchi, L. Fabbrizzi, F. Foti and A. Poggi, *C. R. Chim.*, 2005, **8**, 1519.
38. (a) R. S. Forgan, B. D. Roach, P. A. Wood, F. J. White, J. Campbell, D. K. Henderson, E. Kamenetzky, F. E. McAllister, S. Parsons, E. Pidcock, P. Richardson, R. M. Swart and P. A.

- Tasker, *Inorg. Chem.*, 2011, **50**, 4515; (b) R. S. Forgan, J. E. Davidson, F. P. A. Fabbiani, S. G. Galbraith, D. K. Henderson, S. A. Moggach, S. Parsons, P. A. Tasker and F. J. White, *Dalton Trans.*, 2010, **39**, 1763.
39. (a) J. R. Turkington, V. Cocalia, K. Kendall, C. A. Morrison, P. Richardson, T. Sassi, P. A. Tasker, P. J. Bailey and K. C. Sole, *Inorg. Chem.*, 2012, **51**, 12805; (b) P. V. R. Bhaskara-Sarma and B. R. Reddy, *Miner. Eng.*, 2002, **15**, 461; (c) H. Morizono, T. Oshima and Y. Baba, *Sep. Purif. Technol.*, 2011, **80**, 390; (d) S. Ohmuro, H. Kishi, N. Yoshihara and H. Kokusen, *Talanta*, 2014, **128**, 102.
40. M. Tanaka, K. Koyama and J. Shibata, *Ind. Eng. Chem. Res.*, 1998, **37**, 1943.
41. (a) L. Tijoe, T. Joshi, C. M. Forsyth, B. Moubaraki, K. S. Murray, J. Brugger, B. Graham and L. Spiccia, *Inorg. Chem.*, 2012, **51**, 939.
42. (a) L. M. P. Lima, D. Esteban-Gómez, R. Delgado, C. Platas-Iglesias and R. Tripier, *Inorg. Chem.*, 2012, **51**, 6916; (b) R. D. Hancock, M. S. Shaikjee, S. M. Dobson and J. C. A. Boeyens, *Inorg. Chim. Acta*, 1988, **154**, 229.
43. (a) G. Anderegg, E. Hubmann, N. G. Podder and F. Wenk, *Helv. Chim. Acta*, 1977, **60**, 123; (b) R. Nakon, P. R. Rechani and R. J. Angelici, *J. Am. Chem. Soc.*, 1974, **96**, 2117.
44. (a) L. M. P. Lima, D. Esteban-Gómez, R. Delgado, C. Platas-Iglesias and R. Tripier, *Inorg. Chem.*, 2012, **51**, 6916; (b) R. D. Hancock, M. S. Shaikjee, S. M. Dobson and J. C. A. Boeyens, *Inorg. Chim. Acta*, 1988, **154**, 229.
45. (a) J. K. Romary, J. D. Barger and J. E. Bunds, *Inorg. Chem.*, 1968, **7**, 1142; (b) D. W. Gruenwedel, *Inorg. Chem.*, 1967, **7**, 495.
46. R. S. Forgan, J. E. Davidson, S. G. Galbraith, D. K. Henderson, S. Parsons, P. A. Tasker and F. J. White, *Chem. Commun.*, 2008, 4049.
47. J. Glerup, P. A. Goodson, D. J. Hodgson, K. Michelsen, K. M. Nielsen and H. Weihe, *Inorg. Chem.*, 1992, **31**, 4611.
48. P. Gans, A. Sabatini and A. Vacca, *Talanta*, 1996, **43**, 1739.
49. *SADABS, Bruker-AXS, Version 1*, Bruker AXS Inc., Madison, WI, 2004.
50. G. M. Sheldrick, *Acta Crystallogr., Sect. A: Fundam. Crystallogr.*, 2008, **64**, 112.
51. L. J. Farrugia, *J. Appl. Crystallogr.*, 1999, **32**, 837.
52. DIRDIF99. P. T. Beurskens, G. Beurskens, R. de Gelder, S. García-Granda, R. O. Gould, R. Israel and J. M. M. Smits, *The DIRDIF-99 program system, Technical Report of the Crystallography Laboratory*, University of Nijmegen, The Netherlands, 1999.

† Electronic supplementary information (ESI) available: Bond distances and angles of the metal coordination environments obtained from X-ray measurements, NMR spectra, spectrophotometric titrations, DFT structures and solvent extraction studies. CCDC 1525435–1525438. For ESI and crystallographic data in CIF or other electronic format see DOI: [10.1039/c7dt00093f](https://doi.org/10.1039/c7dt00093f).